
Causal Abstractions of Neural Networks

Atticus Geiger*, Hanson Lu*, Thomas Icard, and Christopher Potts

Stanford

Stanford, CA 94305-2150

{atticusg, hansonlu, icard, cgpotts}@stanford.edu

Abstract

Structural analysis methods (e.g., probing and feature attribution) are increasingly important tools for neural network analysis. We propose a new structural analysis method grounded in a formal theory of *causal abstraction* that provides rich characterizations of model-internal representations and their roles in input/output behavior. In this method, neural representations are aligned with variables in interpretable causal models, and then *interchange interventions* are used to experimentally verify that the neural representations have the causal properties of their aligned variables. We apply this method in a case study to analyze neural models trained on Multiply Quantified Natural Language Inference (MQNLI) corpus, a highly complex NLI dataset that was constructed with a tree-structured natural logic causal model. We discover that a BERT-based model with state-of-the-art performance successfully realizes the approximate causal structure of the natural logic causal model, whereas a simpler baseline model fails to show any such structure, demonstrating that neural representations encode the compositional structure of MQNLI examples.

1 Introduction

Explainability and interpretability have long been central issues for neural networks, and they have taken on renewed importance as such models are now ubiquitous in research and technology. Recent structural evaluation methods seek to reveal the internal structure of these “black box” models. Structural methods include probes, attributions (feature importance methods), and interventions (manipulations of model-internal states). These methods can complement standard behavioral techniques (e.g., performance on gold evaluation sets), and they can yield insights into how and why models make the predictions they do. However, these tools have their limitations, and it has often been assumed that more ambitious and systematic causal analysis of such models is beyond reach.

Although there is a sense in which neural networks are “black boxes”, they have the virtue of being completely closed and controlled systems. This means that standard empirical challenges of causal inference due to lack of observability simply do not arise. The challenge is rather to identify high-level causal regularities that *abstract away* from irrelevant (but arbitrarily observable and manipulable) low-level details. Our contribution in this paper is to show that this challenge can be met. Drawing on recent innovations in the formal theory of causal abstraction [Chalupka et al., 2016, Rubenstein et al., 2017, Beckers and Halpern, 2019, Beckers et al., 2020], we offer a methodology for meaningful causal explanations of neural network behavior.

Our methodology consists of three stages. (1) Formulate a hypothesis by defining a causal model that might explain network behavior. Candidate causal models can be naturally adapted from theoretical and empirical modeling work in linguistics and cognitive sciences. (2) Search for an alignment between neural representations in the network and variables in the high-level causal model. (3) Verify experimentally that the neural representations have the same causal properties as their aligned high-level variables using the *interchange intervention* method of Geiger et al. [2020].

*equal contribution, randomized order

As a case study, we apply this methodology to LSTM-based and BERT-based natural language inference (NLI) models trained on the logically complex Multiply Quantified NLI (MQNLI) dataset of Geiger et al. [2019]. This challenging dataset was constructed with a tree-structured natural logic causal model [MacCartney and Manning, 2007, van Benthem, 2008, Icard and Moss, 2013]. Our BERT-based model has the structure of a standard NLI classifier, and yet it is able to perform well on MQNLI (88%), a result Geiger et al. achieved only with highly customized task-specific models. By contrast, our LSTM-based model is much less successful (46%).

The obvious scientific question in this case study is what drives the success of the BERT-based model on this challenging task. To answer this we employ our methodology. (1) We formulate hypotheses by defining simplified variants of the natural logic causal model. (2) We search over potential alignments between neural representations in BERT and variables in our high-level causal models. (3) We perform interchange interventions on the BERT model for each alignment. We find that our BERT model partially realizes the causal structure of the natural logic causal model; crucially, the LSTM model does not. High-level causal explanation for system behavior is often considered a gold standard for interpretability, one that may be thought quixotic for complex neural models [Lillicrap and Kording, 2019]. The point of our case study is to show that, using the methodology we propose, this high standard can be achieved.

We conclude by comparing our methodology to the probing and the attribution method of integrated gradients [Sundararajan et al., 2017]. We argue that correlational methods such as probing are unable to provide a causal characterization of models. While attribution methods do measure causal properties, our method of aligning neural representations with variables in a causal model provides a richer causal characterization. (We make these arguments formally in Appendix A.)

2 Related Work

Probes Probes are supervised models trained on the internal representations of networks with the goal of determining what those internal representations encode [Hupkes et al., 2018, Peters et al., 2018, Tenney et al., 2019, Clark et al., 2019]. Probes are fundamentally unable to directly measure causal properties of neural representations. We argue this formally in Appendix A.1 by presenting a simple network in which a probe finds information that, by construction, plays no causal role in the network. Ravichander et al. [2020], Elazar et al. [2020], and Geiger et al. [2020] have argued that probes are poor indirect evidence of causal properties as well.

Attribution Methods Attribution methods aim to quantify the degree to which a network representation contributes to the output prediction of the model, for a specific example or set of examples [Zeiler and Fergus, 2014, Springenberg et al., 2014, Shrikumar et al., 2016, Binder et al., 2016, Sundararajan et al., 2017]. Chattopadhyay et al. [2019] develop an attribution method that explicitly treats neural models as structured causal models and computes the individual causal effect of a feature to determine its attribution. While attribution methods certainly measure causal properties, assigning each neural representation a single scalar value is a limited characterization of that representation’s role in network behavior. We address this issue directly in Appendix A.3 by presenting a simple network in which the integrated gradients method [Sundararajan et al., 2017] cannot determine between two neural representations that, by construction, have distinct causal roles in the network.

Interventions Intervention methods actively manipulate the value of neural representations during the network evolution and measure the activity of causally downstream neurons. Several analysis methods use interventions on input representations to provide causal characterizations Feder et al. [2021], Molnar [2019], and some also construct interpretable models from these characterizations Lundberg and Lee [2017], Ribeiro et al. [2016]. Model internal intervention have been used for task-specific analyses [Soulos et al., 2020, Giulianelli et al., 2018, Geiger et al., 2020], but, to our knowledge, only Elazar et al. [2020], Vig et al. [2020], and this paper develop a general methodological approach founded on such interventions.

Causal Abstraction Theories of causal abstraction define when a high-level model faithfully abstracts a low-level model in a way that preserves causal relationships [Chalupka et al., 2016, Rubenstein et al., 2017, Beckers and Halpern, 2019, Beckers et al., 2020]. The notion of abstraction that we employ is here is a relatively simple one called *constructive abstraction* [Beckers and Halpern,

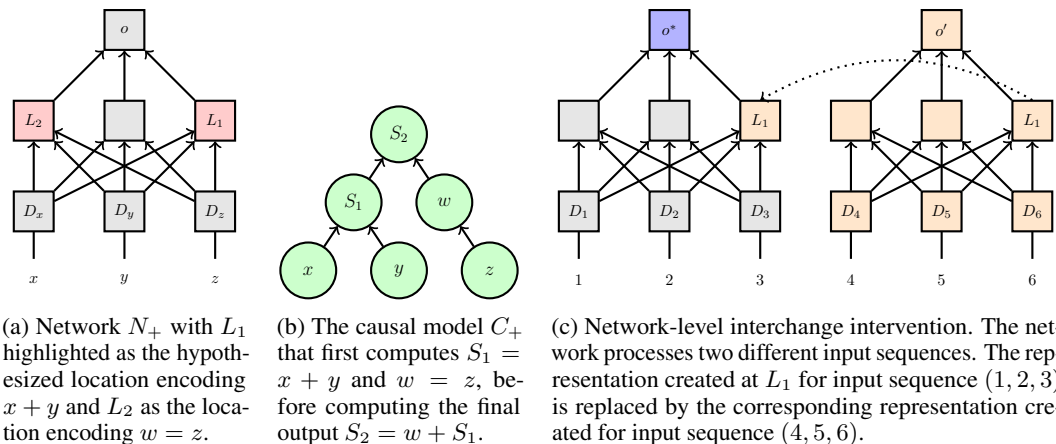


Figure 1: Our motivating example. The interchange intervention method depicted schematically at right can be used to test the hypothesis that the model C_+ is a causal abstraction of the network N_+ .

2019]. Informally, a high-level model is a constructive abstraction of a low-level model if there is a way to partition the variables in the low-level model where each high-level variable can be assigned to a low-level partition cell, such that there is a systematic correspondence between interventions on the low-level partition cells and interventions on the high-level variables.

There are two properties of constructive abstraction that make it ideal for neural network analysis. First, the information content of partitions of low-level variables is determined by the high-level variables that they correspond to. For neural networks, the partitions of low-level variables are sets of neurons, and our method supports reasoning at the level of vector representations (sets of neurons). Second, the causal dependencies between partitions of low-level variables are not necessarily preserved as causal dependencies between the high-level variables corresponding to these partitions. For example, the low-level model might be a fully connected neural network, whereas the high-level model might have much sparser connections. For neural network analysis, this means we can find causal abstractions that have far simpler causal structures than the underlying neural networks. We provide an example in the next section.

3 Causal Abstractions of Neural Networks

We now describe our methodology in more detail, illustrating the relevant concepts with an example of a neural network performing basic arithmetic. Specifically, suppose that we have a neural network N_+ that takes in three vector representations D_x, D_y, D_z representing the integers x, y , and z , and outputs the sum of the three inputs: $N_+(D_x, D_y, D_z) = x + y + z$. We seek an informative causal explanation of this network’s behavior.

Formulating a Hypothesis A human performing this task might follow an algorithm in which they add together the first two numbers and then add that sum to the third number. We can hypothesize that the behavior of N_+ is explained by this algorithm. Specifically, the network combines D_x and D_y to create an internal representation at some location L_1 encoding $a = x + y$; it encodes z at some location L_2 ; and L_1 and L_2 are composed to encode $a + z$ at the location of the output representation. This hypothesis is given schematically in Figure 1a.

Following our methodology, we first define the causal model C_+ in Figure 1b. Our informal hypothesis that a neural network’s behavior is explained by a simple algorithm can then be restated more formally: C_+ is a constructive abstraction of the neural network N_+ .

Alignment Search Now that we have hypothesized that the causal model C_+ is a causal abstraction of the network N_+ , the next step is to align the neural representations in N_+ with the variables in C_+ . The input embeddings D_x, D_y , and D_z must be aligned with the input variables x, y , and z and the output neuron o must be aligned with the output variable S_2 . That leaves the intermediate variables S_1 and w to be aligned with neural representations at some undetermined locations L_1 and L_2 . If

this were an actual experiment (see below), we would perform an *alignment search* to consider many possible values for L_1 and L_2 . Each alignment is a hypothesis about where the network N_+ stores and uses the values of S_1 and w .

Interchange Interventions Finally, for each alignment, we would experimentally determine whether the neural representations at L_1 and L_2 have the same causal properties as S_1 and w . The basic experimental technique we use is an *interchange intervention*, in which a neural representation created during prediction on an input is interchanged with the representation created for a second input [Geiger et al., 2020]. We now show informally that this method can be used to prove that the causal model C_+ is a constructive abstraction of the neural network N_+ (see Appendix H for details).

We first intervene on the causal model. Consider two inputs $\mathbf{a}, \mathbf{a}' \in (\mathbb{N}_9)^3$ where \mathbb{N}_9 is the set of integers 0–9. Let $\mathbf{a} = (x, y, z)$ and $\mathbf{a}' = (x', y', z')$. Define

$$C_+^{S_1 \leftarrow \mathbf{a}'}(\mathbf{a}) = x' + y' + z \quad (1)$$

to be the output provided by C_+ when S_1 , the variable representing the intermediate sum, is intervened on and set to the value $x' + y'$. Thus, for example, if $C_+(1, 2, 3) = 6$, and $\mathbf{a}' = (4, 5, 6)$, then $C_+^{S_1 \leftarrow \mathbf{a}'}(1, 2, 3) = 4 + 5 + 3 = 12$.

Next, we intervene on the neural network N_+ . Let \mathbf{D} be an embedding space that provides unique representations for \mathbb{N}_9 , and consider two inputs $D = (D_x, D_y, D_z)$ and $D' = (D_{x'}, D_{y'}, D_{z'})$, where all D_i and $D_{i'}$ are drawn from \mathbf{D} . In parallel with (1), define

$$N_+^{L_1 \leftarrow D'}(D) \quad (2)$$

to be the output provided by N_+ processing the input D when the representation at location L_1 is replaced with the representation at location L_1 created when N_+ is processing the input D' . This process is depicted in Figure 1c.

With these two definitions, we can define what it means to test the hypothesis that N_+ computes $x + y$ at position L_1 . Where $D_{\mathbf{a}}$ is an embedding for \mathbf{a} and $D_{\mathbf{a}'}$ is an embedding for \mathbf{a}' , we test:

$$C_+^{S_1 \leftarrow \mathbf{a}'}(\mathbf{a}) = N_+^{L_1 \leftarrow D_{\mathbf{a}'}}(D_{\mathbf{a}}) \quad (3)$$

If this equality holds for all \mathbf{a} and \mathbf{a}' , then we can conclude that, for every intervention on S_1 , there is an equivalent intervention on L_1 . If we can establish a corresponding claim for w and L_2 , then we have shown that C_+ is a constructive abstraction of N_+ , since the inputs' relationships are established by our embedding and there are no other interventions on C_+ to test.

Analysis Suppose that all of our intervention experiments verify our hypothesis that C_+ is a constructive abstraction of N_+ with variables S_1 and w aligned to neural representations at L_1 and L_2 . How exactly does this explain network behavior?

Proving the constructive abstraction relation holds with this particular alignment tells us crucial information about the neural representations at L_1 and L_2 , specifically (1) what information is encoded in the representations and (2) the causal role these representations play in network behavior.

Neural representations encode the values of the high-level variables they are aligned with. The location L_1 encodes the value $S_1 = x + y$ and the location L_2 encodes the value w . This is similar to what probing achieves. However, our method is crucially different from probing. In probing, information content is established through purely correlational properties, meaning a neural representation with no causal role in network behavior can be successfully probed. In causal abstraction analysis, information content is established through purely causal properties, ensuring that the neural representation is actually implicated in model behavior.

Neural representations play a parallel causal role to their aligned high-level variables. At the location L_1 , D_x and D_y are composed to form a neural representation with content $x + y$ that is then composed with L_2 to create an output. The fact that S_1 doesn't depend on z tells us that while L_1 depends on D_z and representations at L_1 may even correlate with z , the information about z is not causally represented at L_1 . At the location L_2 , the value of z is simply repeated and then composed with L_1 to create a final output.

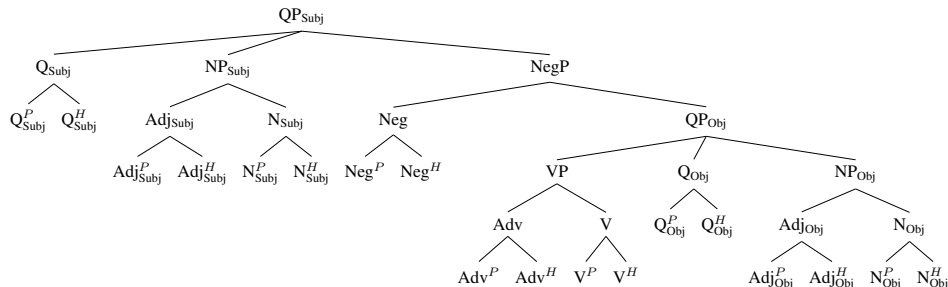


Figure 2: The causal structure of the high-level natural logic causal model C_{NatLog} that performs inference on MQNLI. The superscripts P and H stand for ‘premise’ and ‘hypothesis’ and the subscripts ‘Obj’ and ‘Subj’ stand for ‘subject’ and ‘object’. The node labels are used to explain the experimental results in Section 5 and Section 5.2.

ϵ every ϵ baker $\epsilon \epsilon \epsilon$ eats ϵ no ϵ bread
contradiction
 ϵ no angry baker $\epsilon \epsilon \epsilon$ eats ϵ no ϵ bread
 ϵ every silly professor $\epsilon \epsilon \epsilon$ sells not every ϵ book
neutral
 ϵ every silly professor $\epsilon \epsilon \epsilon$ sells not every ϵ chair
not every sad baker $\epsilon \epsilon$ fairly admits not every odd idea
entailment
 ϵ some ϵ baker does not ϵ admits ϵ no ϵ idea

(a) MQNLI examples. The ϵ token serves as padding (but still attended to by the model) and ensures a perfect alignment between both premises and hypotheses and across all examples. It is semantically an identity element.

Model	Train	Dev	Test
CBoW	88.04	54.18	53.99
TreeNN	67.01	54.01	53.73
CompTreeNN	99.65	80.17	80.21
BiLSTM	99.42	46.41	46.32
BERT	99.99	88.25	88.50

(b) MQNLI results. The first three models are from Geiger et al. 2019, where the CompTreeNN is a task-specific model not suitable for general NLI and functions as an idealized upperbound. Our results show that BERT-based models can surpass this without such alignments.

Table 1: MQNLI examples (left) and MQNLI results (right).

Compare this characterization of the causal roles of neural representations with that provided by attribution methods, which would assign L_1 and L_2 a single scalar value based on their contribution to the final output. This gives us no information about what representations are being composed together at L_1 and L_2 , nor what representations are composed from representations at L_1 and L_2 .

Our method assigns causally impactful information content, but also identifies the abstract causal structure along which representations are composed. It encompasses and improves on correlational and attribution methods.

4 The Natural Language Inference Task and Models

Multiply Quantified NLI Dataset The Multiply Quantified NLI (MQNLI) dataset of Geiger et al. [2019] contains templatically generated English-language NLI examples that involve very complex interactions between quantifiers, negation, and modifiers. We provide a few examples in Table 1a; the emptystring symbol ϵ ensures perfect alignments at the token level both between premises and hypotheses and across all examples.

The MQNLI examples are labeled using an algorithmic implementation of the natural logic of MacCartney and Manning [2009] over tree structures, and the dataset distribution includes a method for creating train/dev/test splits that vary in their difficulty. In the hardest setting, the train set is provably the minimal set of examples required to ensure that the dev and test sets can be perfectly solved by a simple symbolic model; in the easier settings, the train set redundantly encodes necessary information, which might allow a model to perform perfectly in assessment by memorization despite not having found a truly general solution. For a fuller review of the dataset, see Appendix B.

MQNLI is a fitting benchmark given our goals for a few reasons. First, we can focus on the hardest splits that can be generated, which will stress-test our NLI architectures in a standard behavioral way. Second, the MQNLI labeling algorithm is itself a causal model of the data-generating process. Figure 2 summarizes this model in tree form and it is presented in full detail in Geiger et al. [2019]. This allows us to rigorously assess whether a neural network has learned to implement variants of this causal model. The complexity of the MQNLI examples creates many opportunities to do this in linguistically interesting ways.

Models We evaluated two models on MQNLI: a randomly initialized multilayered Bidirectional LSTM (BiLSTM; Schuster and Paliwal [1997]) and a BERT-based classifier model in which the English `bert-base` parameters [Devlin et al., 2019] are fine-tuned on the MQNLI train set. Output predictions are computed using the final representation above the [CLS] token. Models are trained to predict the relation of every pair of aligned phrases in Figure 2. Additional model and training details are given in Appendix C.

Results Table 1b summarizes the results of our BERT and BiLSTM models on the hardest fair generalization task Geiger et al. [2019] creates with MQNLI. We find that our BiLSTM model is not able to learn this task, and that our BERT model is able to achieve high accuracy. The only models in Geiger et al. [2019] able to achieve above 50% accuracy were task specific tree-structured models with the structure of the tree in Figure 2. Thus, our BERT-based model is the first general-purpose model able to achieve good performance on this hard generalization task.

A natural hypothesis is that the BERT-based model achieves this high performance *because* it has in effect induced some approximation to the tree-like structure of the data-generating process in its own internal layers. With the present methodology we are actually in a position to test this hypothesis.

5 A Case Study in Structural Neural Network Analysis

5.1 Causal Abstractions of Neural NLI models

Formulating Our Hypotheses We proceed just as we did for the simple motivating example in Section 3, except that we are now seeking to assess the extent to which the natural logic algebra in Figure 2 is a causal abstraction of the trained neural models in the above section.

The hallmark of Figure 2 is that it defines an alignment between premise and hypothesis at both lexical and phrasal levels. This permits us to run interchange interventions in a naturally compositional way. For a given non-leaf node N in Figure 2, let C_{NatLog}^N be a submodel of C_{NatLog} that computes the relation between the aligned phrases under N and uses them to compute the final output relation between premise and hypothesis. For example, let $C_{NatLog}^{NP_{Obj}}$ be the submodel of C_{NatLog} that computes the relation between the two aligned object phrases and then uses that relation in computing the final output relation between premise and hypothesis. We would like to ask whether our trained neural models also compute this relation between object noun phrases and use it to make a final prediction. We can pose this same question for other nodes which correspond to a pair of aligned subphrases.

Alignment Search For each N , we search for an alignment between a neural representations in N_{NLI} and the variable N in C_{NatLog}^N . In principle, any location in the network could be the right one for any causal model. Testing every hypothesis in this space would be intractable. Thus, for each C_{NatLog}^N , we consider a restricted set of hidden representations based on the identity of N :

- $Q_{Subj}, Adj_{Subj}, N_{Subj}, Neg, Adv, V, Q_{Obj}, Adj_{Obj}, N_{Obj}$: hidden representations above the two descendant leaf tokens.
- QP_{Obj} : hidden representations above Q_{Obj}^P and Q_{Obj}^H .
- $NP_{Subj}, VP, and NP_{Obj}$: same but above the four descendant leaf tokens.
- $NegP$: same but above Neg^P and Neg^H .
- All nodes (for BERT): same but above [CLS] and [SEP].

Interchange Interventions As in Section 3, we first focus on our high-level causal model, in this case Figure 2. Consider a non-leaf node N from Figure 2 and two input token sequences e and e'

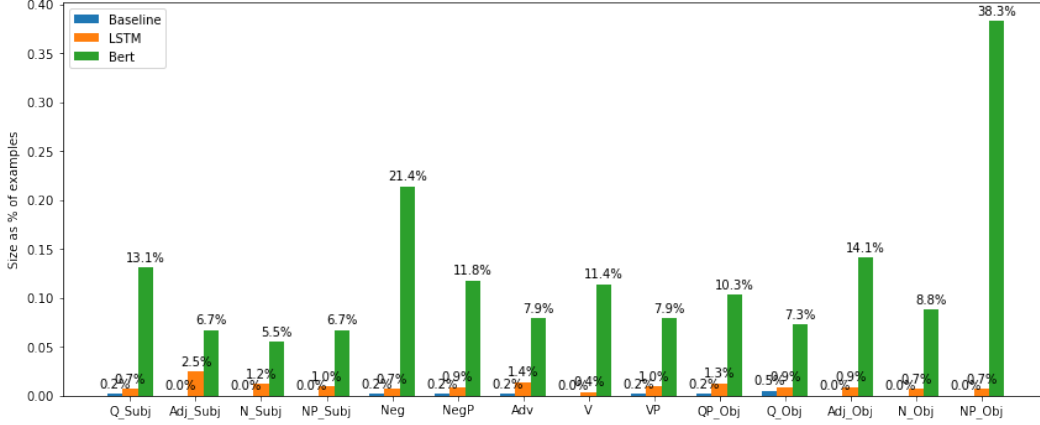


Figure 3: The largest subset of examples on which C_{NatLog}^N is an abstraction of an LSTM and BERT model both trained on MQNLI, and a baseline BERT model with no fine-tuning at all, where N is a non-leaf node of the tree in Figure 2. We record the size of such subsets as a percentage of the total 1000 examples. On this subset, we know that the neural models compute a representation of the relation between the aligned subphrases under N and use this information to make a final prediction.

from MQNLI. Define

$$C_{NatLog}^{N \leftarrow e'}(e) \quad (4)$$

to be the output provided by the causal model C_{NatLog}^N when processing input e where the relation between the aligned subphrases under the node N is changed to the relation between those subphrases in e' . For example, simplifying for the sake of exposition, suppose e is (*every happy person, some happy baker*), which has output label entailment, and suppose e' is (*some happy baker, no ϵ baker*), which has output label contradiction. We wish to intervene on the noun phrase, so $N = NP$. In e , the noun phrase relation is reverse entailment; in e' , it is entailment. Thus, $C_{NatLog}^{NP \leftarrow e'}(e)$ changes the object noun phrase relation in e to entailment while holding everything else about e constant. This results in the output label **neutral**.

Next, we consider interventions in a neural model N_{NLI} . Define

$$N_{NLI}^{L \leftarrow e'}(e) \quad (5)$$

to be the output provided by N_{NLI} processing the input e when the representation at location L is replaced with the representation at location L created when N_{NLI} is processing e' . This is exactly the process depicted in Figure 1a, except now the networks are the complex trained networks of Section 4.

Our hypothesis linking Figure 2 with a model N_{NLI} takes the same form as (3). The causal model C_{NatLog}^N is a constructive abstraction of N_{NLI} when, for some representation location L , it is the case that, for all MQNLI examples e and e' , we have

$$C_{NatLog}^{N \leftarrow e'}(e) = N_{NLI}^{L \leftarrow e'}(e) \quad (6)$$

This asserts a correspondence between interventions on the representations at L in network N_{NLI} and interventions on the variable N in the causal model C_{NatLog}^N . If it holds, then N_{NLI} computes the relation between the aligned phrases under the node N and uses this information to compute the relation between the premise and hypothesis.

We call a pair of examples (e, e') *successful* if it satisfies equation (6), i.e., interventions in both the target causal model and neural model produce equal results. In addition, to isolate the causal impact of our interventions, we specifically focus on pairs (e, e') for which performing the intervention produces a different output value than without the intervention:

$$C_{NatLog}^{N \leftarrow e'}(e) \neq C_{NatLog}^N(e) \quad (7)$$

We call a pair (e, e') *impactful* if it satisfies (7).

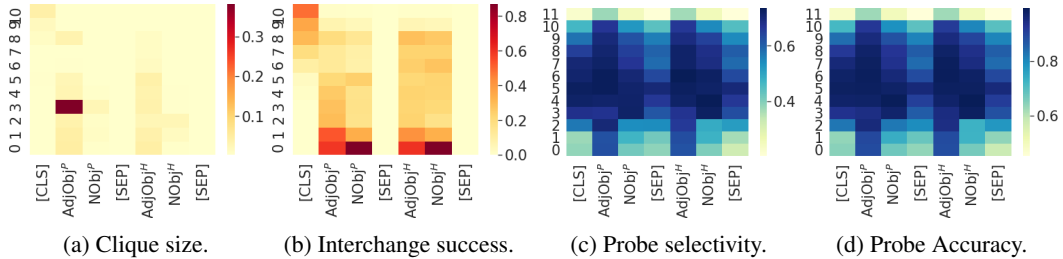


Figure 4: Interchange intervention and probing results for the NP_{Obj} position. Vertical axes denote layers of BERT and horizontal axes denote the token position of hidden representations. The intervention success rates reported here are calculated based on intervention experiments with a change in the output label. Clique sizes are reported as % of 1000 examples. We did not conduct interchange experiments on the layer 11 of BERT because all representations on this layer except the one above [CLS] causally affected the result.

Quantifying Partial Success Equation (6) universally quantifies over all examples. We do not expect this kind of perfect correspondence to emerge in practice for real problems: neural network training is often approximate and variable in nature, and even our best model does not achieve *perfect* performance. However, we can still ask how widely (6) holds for a given model. To do this, we seek to find the *largest subset* of MQNLI on which C_{NatLog}^N is an abstraction of our neural models, for each non-leaf node N in C_{NatLog} .

More specifically, considering each example in MQNLI as a vertex in a graph, we add an undirected edge between two examples e_i, e_j if and only if both the ordered pairs (e_i, e_j) and (e_j, e_i) satisfy (6). In other words, C_{NatLog}^N is an abstraction of a neural model on a subset of examples S of MQNLI if and only if all examples in S form a *clique*.

The number of intervention experiments we need to run scales quadratically with the number of inputs we consider, so we sample 1000 MQNLI examples, producing a total of $1000 \times 1000 = 1\text{M}$ ordered pairs. We only consider examples for which that the neural network outputs a correct label. For each node N and each of its corresponding neural network locations L , we perform interventions on all of these pairs.

Results and Analysis For each target causal model node N and neural network representation location L , we construct a graph as described above with 1000 examples as vertices and add an edge between two examples e_i and e_j if and only if *both* (e_i, e_j) and (e_j, e_i) are successful. We then find the largest clique in this graph with at least one impactful edge and record its size.

Figure 3 shows, for each causal model node N , the maximum size of cliques found among all neural locations. With this stricter *impactful* criterion (as opposed to simply using intervention success), our results show that, for almost all nodes N our target causal model, C_{NatLog}^N is indeed a causal abstraction of BERT, on a significant number of examples in our dataset. These subsets are much smaller for the BiLSTM model.

We will now explain what these successful results tell us about (1) the information encoded by representations, and (2) the causal role these representations play in network behavior.

This analysis is similar to the analysis of our hypothetical addition example in Section 3, except for two crucial differences. First, for each variable N , we are hypothesizing that the causal model C_{NatLog}^N is an abstraction of N_{NLI} , whereas in the addition example there was only one model. To account for this difference, we will be taking $N = \text{NP}_{\text{Obj}}$ as a paradigm case, with the results an analysis for other nodes in Appendix D. Second, we only achieved partial experimental success, whereas in the addition example we assumed complete success. Crucially, this means that the following analysis will only be valid on subsets of the input space on which the abstraction relation holds between N_{NLI} and $C_{\text{NatLog}}^{\text{NP}_{\text{Obj}}}$.

We visualize the results of our intervention experiments for the node NP_{Obj} in Figure 4. Observe that the alignment with the largest subset of inputs aligns the NP_{Obj} variable in $C_{\text{NatLog}}^{\text{NP}_{\text{Obj}}}$ with the neural representation on the fourth layer of BERT above the $\text{Adj}_{\text{Obj}}^P$ token. Because neural representations

encode the value of their aligned variables and play a parallel causal role to their high-level variables, we know that, on this subset of input examples, at the fourth neural representation above the $\text{Adj}_{\text{Obj}}^P$ token, the four input embeddings for the object nouns and adjectives in the premise and hypothesis are composed to form a neural representation with information content of the relation between the object noun phrases in the premise and hypothesis. Then this representation is composed with the other input-embeddings to create an output representing the relation between the premise and hypothesis. We can perform a similar analysis for every other high-level variable, using the heatmaps from Appendix D.

We additionally would like to acknowledge that focusing on MQNLI could reinforce normative notions of how English is used and how reasoning in language works that could be exclusionary.

5.2 Comparison with Other Structural Analysis Methods

Probes Probes are fundamentally unable to measure causal properties of representations, instead determining the information content of representations using a modified measure of the correlation between neural representations and symbolic variables. We probed neural representation locations for the relation between aligned subexpressions on a subset of 12,800 randomly selected MQNLI examples. For a pair of aligned subexpressions below a node N in Figure 2, we probe the columns above the same set of restricted class of tokens as described in Section 5.1.

To evaluate these probes, we report accuracy as well as *selectivity* as defined by Hewitt and Liang [2019]: probe accuracy minus control accuracy, where *control accuracy* is the train set accuracy of a probe with the same architecture but trained on a control task to factor out probe success that can be attributed to the probe model itself. Our control task is to learn a random mapping from node types to semantic relations; see Appendix F for full details on how this task was constructed.

Figure 4 summarizes our probing results for $N = \text{NP}_{\text{Obj}}$, along with corresponding interchange intervention results for comparison. Probes tell us that information about the relation between the aligned noun phrases is encoded in nearly all of the locations we considered, and using the selectivity metric does not result in any qualitative change. In contrast, our intervention heatmaps indicate only a small number of locations store this information in a causally relevant way. Clearly, our intervention experiments are far more discriminating than probes. Appendix D provides examples involving other variables along with the intervention experiments, where the general trend of interchange interventions being more discriminate holds.

Integrated Gradients Attribution methods that estimate feature importance can measure causal properties of neural representations (see Appendix A.2), but a single feature importance method is an impoverished characterization of a the representations role in network behavior. Whereas our interchange interventions gave us high-level information about how a neural representation is composed and what it is composed into, attribution methods simply tell us “how much” a representation contributes to the network output on a give input. Moreover, intervention interchanges provide a rich, high-level characterization of causal structure on a space of inputs.

We use integrated gradients on our models to verify the intuitive hypothesis that if a premise and hypothesis differ by a single token, then the neural representations above that token should be more causally responsible for the network output than other representations. For example, given premise ‘Every sleepy cat meows’ and hypothesis ‘Some hungry cat meows’ the attributive modifier position is different and the rest are matched. The neural representations above the adjective tokens *sleepy* and *hungry* should be more important for the network output than others, because if those adjectives were the same, the example label would change from **neutral** to **entailment**.

We summarize the results of our integrated gradient experiments in Appendix E, where we confirm our intuitive hypothesis. The results are consistent with the results of our interchange interventions, as locations that had successful interchange interventions were locations where large attribution was assigned, and locations that did not have success were above locations where small attribution was assigned. However, our intervention experiments characterized the *information content* of neural representations and the high-level graph structure along which they are composed.

6 Conclusion

We have introduced a methodology for deriving interpretable causal explanations of neural network behaviors, grounded in a formal theory of causal abstraction. The methodology involves first *formulating a hypothesis* in the form of a high-level, interpretable causal model, then *searching for an alignment* between the neural network and the causal model, and finally *verifying experimentally* that the neural representations encode the same causal properties and information content as the corresponding components of the high-level causal model. As a case study demonstrating the feasibility of the approach, we analyzed neural models trained on the formidable MQNLI dataset. Guided by the intuition that success on this challenging task may call for a way of recapitulating the causal structure of the natural logic model that generates the MQNLI data, we were able to verify the hypothesis that a state-of-the-art BERT-based model partially realizes this structure, whereas baseline models that do not perform as well fail to do so. This suggestive case study demonstrates that our theoretically grounded methodology can work in practice.

Acknowledgements

Our thanks to Noah Goodman and Josh Rozner for valuable input on an earlier version of this paper. This research is supported in part by faculty research grants from Facebook and Google.

References

- S. Beckers and J. Y. Halpern. Abstracting causal models. *Proceedings of the AAAI Conference on Artificial Intelligence*, 33(01):2678–2685, Jul. 2019. doi: 10.1609/aaai.v33i01.33012678. URL <https://ojs.aaai.org/index.php/AAAI/article/view/4117>.
- S. Beckers, F. Eberhardt, and J. Y. Halpern. Approximate causal abstractions. In R. P. Adams and V. Gogate, editors, *Proceedings of The 35th Uncertainty in Artificial Intelligence Conference*, volume 115 of *Proceedings of Machine Learning Research*, pages 606–615, Tel Aviv, Israel, 22–25 Jul 2020. PMLR. URL <http://proceedings.mlr.press/v115/beckers20a.html>.
- A. Binder, G. Montavon, S. Bach, K. Müller, and W. Samek. Layer-wise relevance propagation for neural networks with local renormalization layers. *CoRR*, abs/1604.00825, 2016. URL <http://arxiv.org/abs/1604.00825>.
- S. Bongers, P. Forré, J. Peters, B. Schölkopf, and J. M. Mooij. Foundations of structural causal models with cycles and latent variables. *arXiv.org preprint*, arXiv:1611.06221v4 [stat.ME], Oct. 2020. URL <https://arxiv.org/abs/1611.06221v4>.
- K. Chalupka, F. Eberhardt, and P. Perona. Multi-level cause-effect systems. In A. Gretton and C. C. Robert, editors, *Proceedings of the 19th International Conference on Artificial Intelligence and Statistics*, volume 51 of *Proceedings of Machine Learning Research*, pages 361–369, Cadiz, Spain, 09–11 May 2016. PMLR. URL <http://proceedings.mlr.press/v51/chalupka16.html>.
- A. Chattopadhyay, P. Manupriya, A. Sarkar, and V. N. Balasubramanian. Neural network attributions: A causal perspective. In K. Chaudhuri and R. Salakhutdinov, editors, *Proceedings of the 36th International Conference on Machine Learning*, volume 97 of *Proceedings of Machine Learning Research*, pages 981–990, Long Beach, California, USA, 09–15 Jun 2019. PMLR. URL <http://proceedings.mlr.press/v97/chattopadhyay19a.html>.
- K. Clark, U. Khandelwal, O. Levy, and C. D. Manning. What does BERT look at? an analysis of BERT’s attention. In *Proceedings of the 2019 ACL Workshop BlackboxNLP: Analyzing and Interpreting Neural Networks for NLP*, pages 276–286, Florence, Italy, Aug. 2019. Association for Computational Linguistics. doi: 10.18653/v1/W19-4828. URL <https://www.aclweb.org/anthology/W19-4828>.
- J. Devlin, M.-W. Chang, K. Lee, and K. Toutanova. BERT: Pre-training of deep bidirectional transformers for language understanding. In *Proceedings of the 2019 Conference of the North*

- American Chapter of the Association for Computational Linguistics: Human Language Technologies, Volume 1 (Long and Short Papers)*, pages 4171–4186, Minneapolis, Minnesota, June 2019. Association for Computational Linguistics. doi: 10.18653/v1/N19-1423. URL <https://www.aclweb.org/anthology/N19-1423>.
- Y. Elazar, S. Ravfogel, A. Jacovi, and Y. Goldberg. Amnesic probing: Behavioral explanation with amnesic counterfactuals. In *Proceedings of the 2020 EMNLP Workshop BlackboxNLP: Analyzing and Interpreting Neural Networks for NLP*. Association for Computational Linguistics, Nov. 2020. doi: 10.18653/v1/W18-5426.
- A. Feder, N. Oved, U. Shalit, and R. Reichart. CausaLM: Causal Model Explanation Through Counterfactual Language Models. *Computational Linguistics*, pages 1–54, 05 2021. ISSN 0891-2017. doi: 10.1162/coli_a_00404. URL https://doi.org/10.1162/coli_a_00404.
- A. Geiger, I. Cases, L. Karttunen, and C. Potts. Posing fair generalization tasks for natural language inference. In *Proceedings of the 2019 Conference on Empirical Methods in Natural Language Processing and the 9th International Joint Conference on Natural Language Processing (EMNLP-IJCNLP)*, pages 4475–4485, Stroudsburg, PA, November 2019. Association for Computational Linguistics. doi: 10.18653/v1/D19-1456. URL <https://www.aclweb.org/anthology/D19-1456>.
- A. Geiger, K. Richardson, and C. Potts. Neural natural language inference models partially embed theories of lexical entailment and negation. In *Proceedings of the Third BlackboxNLP Workshop on Analyzing and Interpreting Neural Networks for NLP*, pages 163–173, Online, Nov. 2020. Association for Computational Linguistics. doi: 10.18653/v1/2020.blackboxnlp-1.16. URL <https://www.aclweb.org/anthology/2020.blackboxnlp-1.16>.
- M. Giulianelli, J. Harding, F. Mohnert, D. Hupkes, and W. Zuidema. Under the hood: Using diagnostic classifiers to investigate and improve how language models track agreement information. In *Proceedings of the 2018 EMNLP Workshop BlackboxNLP: Analyzing and Interpreting Neural Networks for NLP*, pages 240–248, Brussels, Belgium, Nov. 2018. Association for Computational Linguistics. doi: 10.18653/v1/W18-5426. URL <https://www.aclweb.org/anthology/W18-5426>.
- J. Hewitt and P. Liang. Designing and interpreting probes with control tasks. In *Proceedings of the 2019 Conference on Empirical Methods in Natural Language Processing and the 9th International Joint Conference on Natural Language Processing (EMNLP-IJCNLP)*, pages 2733–2743, Hong Kong, China, Nov. 2019. Association for Computational Linguistics. doi: 10.18653/v1/D19-1275. URL <https://www.aclweb.org/anthology/D19-1275>.
- D. Hupkes, S. Bouwmeester, and R. Fernández. Analysing the potential of seq-to-seq models for incremental interpretation in task-oriented dialogue. In *Proceedings of the 2018 EMNLP Workshop BlackboxNLP: Analyzing and Interpreting Neural Networks for NLP*, pages 165–174, Brussels, Belgium, Nov. 2018. Association for Computational Linguistics. doi: 10.18653/v1/W18-5419. URL <https://www.aclweb.org/anthology/W18-5419>.
- T. F. Icard and L. S. Moss. Recent progress on monotonicity. *Linguistic Issues in Language Technology*, 9(7):1–31, January 2013.
- G. W. Imbens and D. B. Rubin. *Causal inference in statistics, social, and biomedical sciences*. Cambridge University Press, 2015.
- P.-J. Kindermans, S. Hooker, J. Adebayo, M. Alber, K. T. Schütt, S. Dähne, D. Erhan, and B. Kim. The (un)reliability of saliency methods. In W. Samek, G. Montavon, A. Vedaldi, L. K. Hansen, and K.-R. Müller, editors, *Explainable AI: Interpreting, Explaining and Visualizing Deep Learning*, pages 267–280. Springer, 2019.
- T. P. Lillicrap and K. P. Kording. What does it mean to understand a neural network?, 2019.
- S. M. Lundberg and S.-I. Lee. A unified approach to interpreting model predictions. In I. Guyon, U. V. Luxburg, S. Bengio, H. Wallach, R. Fergus, S. Vishwanathan, and R. Garnett, editors, *Advances in Neural Information Processing Systems*, volume 30. Curran Associates, Inc., 2017. URL <https://proceedings.neurips.cc/paper/2017/file/8a20a8621978632d76c43dfd28b67767-Paper.pdf>.

- B. MacCartney and C. D. Manning. Natural logic for textual inference. In *Proceedings of the ACL-PASCAL Workshop on Textual Entailment and Paraphrasing*, RTE '07, pages 193–200, Stroudsburg, PA, USA, 2007. Association for Computational Linguistics. URL <http://dl.acm.org/citation.cfm?id=1654536.1654575>.
- B. MacCartney and C. D. Manning. An extended model of natural logic. In *Proceedings of the Eight International Conference on Computational Semantics*, pages 140–156, Tilburg, The Netherlands, Jan. 2009. Association for Computational Linguistics. URL <https://www.aclweb.org/anthology/W09-3714>.
- C. Molnar. *Interpretable Machine Learning*. 2019. <https://christophm.github.io/interpretable-ml-book/>.
- M. Peters, M. Neumann, L. Zettlemoyer, and W.-t. Yih. Dissecting contextual word embeddings: Architecture and representation. In *Proceedings of the 2018 Conference on Empirical Methods in Natural Language Processing*, pages 1499–1509, Brussels, Belgium, Oct.-Nov. 2018. Association for Computational Linguistics. doi: 10.18653/v1/D18-1179. URL <https://www.aclweb.org/anthology/D18-1179>.
- A. Ravichander, Y. Belinkov, and E. Hovy. Probing the probing paradigm: Does probing accuracy entail task relevance?, 2020.
- M. Ribeiro, S. Singh, and C. Guestrin. “why should I trust you?”: Explaining the predictions of any classifier. In *Proceedings of the 2016 Conference of the North American Chapter of the Association for Computational Linguistics: Demonstrations*, pages 97–101, San Diego, California, June 2016. Association for Computational Linguistics. doi: 10.18653/v1/N16-3020. URL <https://www.aclweb.org/anthology/N16-3020>.
- P. K. Rubenstein, S. Weichwald, S. Bongers, J. M. Mooij, D. Janzing, M. Grosse-Wentrup, and B. Schölkopf. Causal consistency of structural equation models. In *Proceedings of the 33rd Conference on Uncertainty in Artificial Intelligence (UAI)*. Association for Uncertainty in Artificial Intelligence (AUAI), Aug. 2017. URL <http://auai.org/uai2017/proceedings/papers/11.pdf>. *equal contribution.
- M. Schuster and K. K. Paliwal. Bidirectional recurrent neural networks. *IEEE transactions on Signal Processing*, 45(11):2673–2681, 1997.
- A. Shrikumar, P. Greenside, A. Shcherbina, and A. Kundaje. Not just a black box: Learning important features through propagating activation differences. *CoRR*, abs/1605.01713, 2016. URL <http://arxiv.org/abs/1605.01713>.
- P. Soulos, R. T. McCoy, T. Linzen, and P. Smolensky. Discovering the compositional structure of vector representations with role learning networks. In *Proceedings of the Third BlackboxNLP Workshop on Analyzing and Interpreting Neural Networks for NLP*, pages 238–254, Online, Nov. 2020. Association for Computational Linguistics. doi: 10.18653/v1/2020.blackboxnlp-1.23. URL <https://www.aclweb.org/anthology/2020.blackboxnlp-1.23>.
- J. Springenberg, A. Dosovitskiy, T. Brox, and M. Riedmiller. Striving for simplicity: The all convolutional net. *CoRR*, 12 2014.
- M. Sundararajan, A. Taly, and Q. Yan. Axiomatic attribution for deep networks. In D. Precup and Y. W. Teh, editors, *Proceedings of the 34th International Conference on Machine Learning*, volume 70 of *Proceedings of Machine Learning Research*, pages 3319–3328, International Convention Centre, Sydney, Australia, 06–11 Aug 2017. PMLR. URL <http://proceedings.mlr.press/v70/sundararajan17a.html>.
- I. Tenney, D. Das, and E. Pavlick. BERT rediscovers the classical NLP pipeline. In *Proceedings of the 57th Annual Meeting of the Association for Computational Linguistics*, pages 4593–4601, Florence, Italy, July 2019. Association for Computational Linguistics. doi: 10.18653/v1/P19-1452. URL <https://www.aclweb.org/anthology/P19-1452>.
- J. van Benthem. A brief history of natural logic. In M. Chakraborty, B. Löwe, M. Nath Mitra, and S. Sarukki, editors, *Logic, Navya-Nyaya and Applications: Homage to Bimal Matilal*, 2008.

- J. Vig, S. Gehrmann, Y. Belinkov, S. Qian, D. Nevo, Y. Singer, and S. Shieber. Causal mediation analysis for interpreting neural nlp: The case of gender bias, 2020.
- T. Wolf, L. Debut, V. Sanh, J. Chaumond, C. Delangue, A. Moi, P. Cistac, T. Rault, R. Louf, M. Funtowicz, and J. Brew. Huggingface’s transformers: State-of-the-art natural language processing. *ArXiv*, abs/1910.03771, 2019.
- M. D. Zeiler and R. Fergus. Visualizing and understanding convolutional networks. In D. Fleet, T. Pajdla, B. Schiele, and T. Tuytelaars, editors, *Computer Vision – ECCV 2014*, pages 818–833, Cham, 2014. Springer International Publishing. ISBN 978-3-319-10590-1.

Supplementary Materials

A The Limits of Probing and Attribution Methods

A.1 Probing Success without Causal Impact

In Section 3, we observed that successful probing does not entail causality. This section presents an analytic example of this. We assume the structure of the N_+ network in Figure 1a. For our embedding, we simply map every integer i in \mathbb{N}_0 to the 1-dimensional vector $[i]$. The weight matrices are

$$W_1 = \begin{pmatrix} 1 \\ 1 \\ 0 \end{pmatrix} \quad W_2 = \begin{pmatrix} 1 \\ 1 \\ 1 \end{pmatrix} \quad W_3 = \begin{pmatrix} 0 \\ 0 \\ 1 \end{pmatrix}$$

and the output weights

$$\mathbf{w} = \begin{pmatrix} 0 \\ 1 \\ 0 \end{pmatrix}$$

The output for an input sequence $\mathbf{x} = (i, j, k)$ is given by

$$(\mathbf{x}W_1; \mathbf{x}W_2; \mathbf{x}W_3) \mathbf{w}$$

In this network, $\mathbf{x}W_1$ perfectly encodes $i + j$, and $\mathbf{x}W_3$ perfectly encodes k . Thus, the identity model probe will be perfect in probing those representations for this information. However, neither representation plays a causal role in the network behavior; only $\mathbf{x}W_2$ contributes to the output.

A.2 Causal Interpretation of Integrated Gradients

In contrast to probing, the integrated gradients method (IG) does have an unambiguous causal interpretation, which we explain here. Following Sundararajan et al. [2017] we define the vector $IG(\mathbf{x})$, for an input \mathbf{x} relative to a baseline \mathbf{b} , to have i th component:

$$(x_i - b_i) \cdot \int_{\alpha=0}^1 \frac{\partial F(\alpha\mathbf{x} + (1-\alpha)\mathbf{b})}{\partial x_i} d\alpha \quad (8)$$

In the cases we consider here, \mathbf{b} is always taken in to be the zero vector, in which case (8) simplifies:

$$x_i \cdot \int_{\alpha=0}^1 \frac{\partial F(\alpha\mathbf{x})}{\partial x_i} d\alpha$$

Let us abbreviate the weighted average vector $\alpha\mathbf{x} + (1-\alpha)\mathbf{b}$ by \mathbf{x}^α , and let $\mathbf{x}^{\alpha,\epsilon}$ be the vector that differs from \mathbf{x}^α in that the i th coordinate is increased by ϵ . Then, simply by expanding the definition of partial derivative, (8) can be rewritten in the following form:

$$(x_i - b_i) \cdot \int_{\alpha=0}^1 \lim_{\epsilon \rightarrow 0} \frac{F(\mathbf{x}^{\alpha,\epsilon}) - F(\mathbf{x}^\alpha)}{\epsilon} d\alpha \quad (9)$$

The difference $F(\mathbf{x}^{\alpha,\epsilon}) - F(\mathbf{x}^\alpha)$ is known as the (individual) *causal effect* on the output (see, e.g., Imbens and Rubin 2015), of increasing neuron i by ϵ relative to the fixed input $\alpha\mathbf{x} + (1-\alpha)\mathbf{b}$. So essentially $IG_i(\mathbf{x})$ is measuring the average “limiting” causal effect of increasing neuron i along the straight line from the baseline vector to the input vector \mathbf{x} , weighted by the difference at i between input and baseline.

Some authors (see Chattopadhyay et al. 2019) have advocated for directly taking the *average* causal effect of an input neuron on an output. This is argued to mitigate interactions between input neurons, as described in Kindermans et al. [2019]. As we show next, the values in (9) do not tell us everything we may want to know about causal structure.

A.3 Equal Attribution to Neural Representations with Distinct Causal Roles

This section presents an analytic example of two neural representations with different causal roles being assigned the same integrated gradient value. Crucially, we are not implying that this is a flaw

with integrated gradients. We are simply pointing out that assigning neural representations a single “causal impact” value has expressive limitations.

We again assume the structure of the network N_+ in Figure 1a, except now we are considering the case when four integer inputs from \mathbb{N}_9 are being added together. For our embedding, we simply map every integer i in \mathbb{N}_9 to the 1-dimensional vector $[i]$. The weight matrices are

$$W_1 = \begin{pmatrix} 1 \\ 1 \\ 0 \\ 0 \end{pmatrix} \quad W_2 = \begin{pmatrix} 0 \\ 0 \\ 1 \\ 1 \end{pmatrix} \quad W_3 = \begin{pmatrix} 0 \\ 0 \\ 0 \\ 0 \end{pmatrix}$$

and the output weights

$$\mathbf{w} = \begin{pmatrix} 1 \\ 1 \\ 0 \end{pmatrix}$$

The output for an input sequence $\mathbf{x} = (3, 4, 5, 2)$ is given by

$$(\mathbf{x}W_1; \mathbf{x}W_2; \mathbf{x}W_3) \mathbf{w}$$

In this network, $\mathbf{x}W_1$ perfectly encodes $3 + 4 = 7$, and $\mathbf{x}W_2$ perfectly encodes $5 + 2 = 7$. Both of these values equally contribute to the final output of 14 because they both have a weight of 1 in the output weights. This means that integrated gradients would assign the neuron $\mathbf{x}W_1$ a value of 7 and the neuron $\mathbf{x}W_2$ a value of 7. From the perspective of IG, these two nodes are indistinguishable. However, intuitively, these nodes are very different from one another. The node $\mathbf{x}W_1$ is composed from the first two inputs and the node $\mathbf{x}W_2$ is composed from the second two inputs. Integrated gradients tells us “how much” a neuron causes the output, but that does not give us information about the high-level structure along which neural representations are composed.

B Additional Details on MQNLI

B.1 Dataset Description

The MQNLI dataset contains sentences of the form

$$Q_S \text{ Adj}_S N_S \text{ Neg Adv V } Q_O \text{ Adj}_O N_O$$

where N_S and N_O are nouns, V is a verb, Adj_S and Adj_O are adjectives, and Adv is an adverb. These categories all have 100 words. Neg is *does not*, and Q_S and Q_O can be *every*, *not every*, *some*, or *no*. Additionally, Adj_S , Adj_O , Adv , and Neg can be the empty string ε .

NLI examples are constructed so that non-identical non-empty nouns, adjectives, verbs, and adverbs with identical positions in s_p and s_h are semantically unrelated. This means that the learning task is trivial for these lexical items, as the correct relation is equivalence when they are identical and independence when they are not identical.

For our experiments, we used a train set with 500K examples, a dev set with 60k examples, and a test set with 10K examples using the most difficult generalization scheme of Geiger et al. [2019].

B.2 A Natural Logic Causal Model

Geiger et al. [2019] construct a natural logic model that solves MQNLI using a formalization they call *composition trees* which is easily translated into the causal model we call C_{NatLog} . Natural logic is a flexible approach to doing logical inference directly on natural language expressions [MacCartney and Manning, 2007, van Benthem, 2008, Icard and Moss, 2013] where the *semantic relations* between phrases are compositionally computed from the semantic relations between aligned subphrases and *projectivity signatures*, which encode how semantic operators interact compositionally with their arguments. The causal model C_{NatLog} performs inference on aligned semantic parse trees that represent both the premise and hypothesis as a single structure and calculates semantic relations between all subphrases compositionally.

Model	Dev	Test
finetuned BERT	88.25	88.50
- augmented examples	55.42	54.51

Table 2: Ablation results

C Model Training and Interchange Experiment Details

We evaluated two models on MQNLI: A multi-layered bidirectional LSTM baseline and a Transformer model trained to do masked language modeling and next-sentence prediction [Devlin et al., 2019]. We rely on the uncased BERT-base initial parameters from Hugging Face `transformers` [Wolf et al., 2019]. For both models, we concatenate the premise s_p and hypothesis s_h into one string with special separator tokens: [CLS] s_p [SEP] s_h [SEP].

For the BiLSTM, we concatenate the hidden state of above the last [SEP] and the [CLS] in the last layer for the forward and backward directions respectively to obtain a representation for the whole input, and then apply three linear transformations on top of it. The final transformation outputs a logit score for each class in the label space.

For the BERT model, we apply one linear transformation to the final layer’s hidden representation above the [CLS] token to obtain a logit score for each label class.

C.1 Tokenization

In the original setting of MQNLI, some positions in the premise and hypothesis as shown in the beginning of Section B.1 consist of two words such as *not every* in Q_S and Q_O and *does not* in the leaf nodes Neg^P and Neg^H . We treat them as two separate tokens in order to utilize BERT’s knowledge of these function words. To ensure all sentences have identical length, we introduce one extra empty string tokens ε to single-word quantifiers and two such tokens in the place of Neg^P and Neg^H for sentences without negation.

For consistency, we use the same tokenization method for both models.

C.2 Dataset Augmentation with Labeled Subphrases

The *hard but fair* MQNLI generalization task requires the dataset to explicitly expose the model to labels for each intermediate node that is a relation in C_{NatLog} . For each training example $(s_p, s_h, y) \in \mathcal{S}$, we augment an additional example (s_p^N, s_h^N, y^N) for each node N . (s_p^N, s_h^N) is the pair of subphrases made up of the leaf tokens under node N in the original (s_p, s_h) , and y^N is the relation computed by C_{NatLog} for the subphrase pair. We use a set of labels for these subphrases examples that is disjoint from that of the full-sentence examples. During training, the augmented examples coupled with original examples in each batch. For BERT, the subphrase pairs occupy their original positions in the sentence while we pad and apply an attention mask over all other positions. For the BiLSTM, we align them to the left, with [SEP] in between the two parts of the pair.

We performed an ablation experiment to test whether removing the augmented examples would affect BERT’s performance. Using the same grid search setting, we see that BERT’s dev set accuracy decreased from 88.25% to 55.42%, and test set accuracy decreased from 88.50% to 54.51%. This indeed shows that the above data augmentation method is important for BERT to learn the type of generalization required for the hard MQNLI task.

C.3 Training Procedure

For the BiLSTM, we use 256 dimensions for token embeddings and 128 dimensions for the hidden states in each LSTM direction. We grid search for $\{2, 4, 6\}$ layers. We randomly initialize each element in the token embeddings from the distribution $\mathcal{N}(0, 1)$ scaled down by a factor of 0.1. We use a batch size of $768 = 64 \times 12$, with 64 original examples per batch and 11 augmented examples for each one. We apply a dropout of 0.1, and grid search for learning rates in $\{0.001, 0.0001\}$. We train for a maximum of 400 epochs and perform early stopping when the development set accuracy

does not increase for 20 epochs. We train each grid search setting 3 times with different random seeds.

For BERT, we use the same model architecture for the uncased base variant. We use a batch size of $192 = 16 \times 12$, and grid search for learning rates in $\{2.0 \times 10^{-5}, 5.0 \times 10^{-5}\}$. We train for a maximum of $\{3, 4\}$ epochs. We warm up the learning rate linearly from 0 to the specified value in the first 25% steps of the first epoch, and linearly decrease the learning rate to 0 following that until the end of training.

All models were trained with 1 GPU core on a cluster with models including GeForce RTX 2080 Ti, GeForce GTX Titan X, Titan XP and Titan V, each with 11-12GB memory. Each instance of the grid search took on average 5.5 hours to train. We repeated each grid search setting with 4 different random seeds.

C.4 Interchange experiment details

There are 14 intermediate nodes in the high-level causal model, (NegP, QP_{Obj}, Q_{Subj}, NP_{Subj}, Adj_{Subj}, N_{Subj}, Neg, VP, Adv, V, Q_{Obj}, NP_{Obj}, Adj_{Obj}, N_{Obj}), and for each high-level node, we conducted a set of interchange experiments on each one of 11 BERT layers (excluding the final layer). Each BERT layer has a varying number of possible hidden locations that were intervened on. For each of the $14 \times 11 = 154$ interchange experiments, it took on average 1.15 hours to run using the same computation resources mentioned above.

D Probing and Intervention Heatmaps

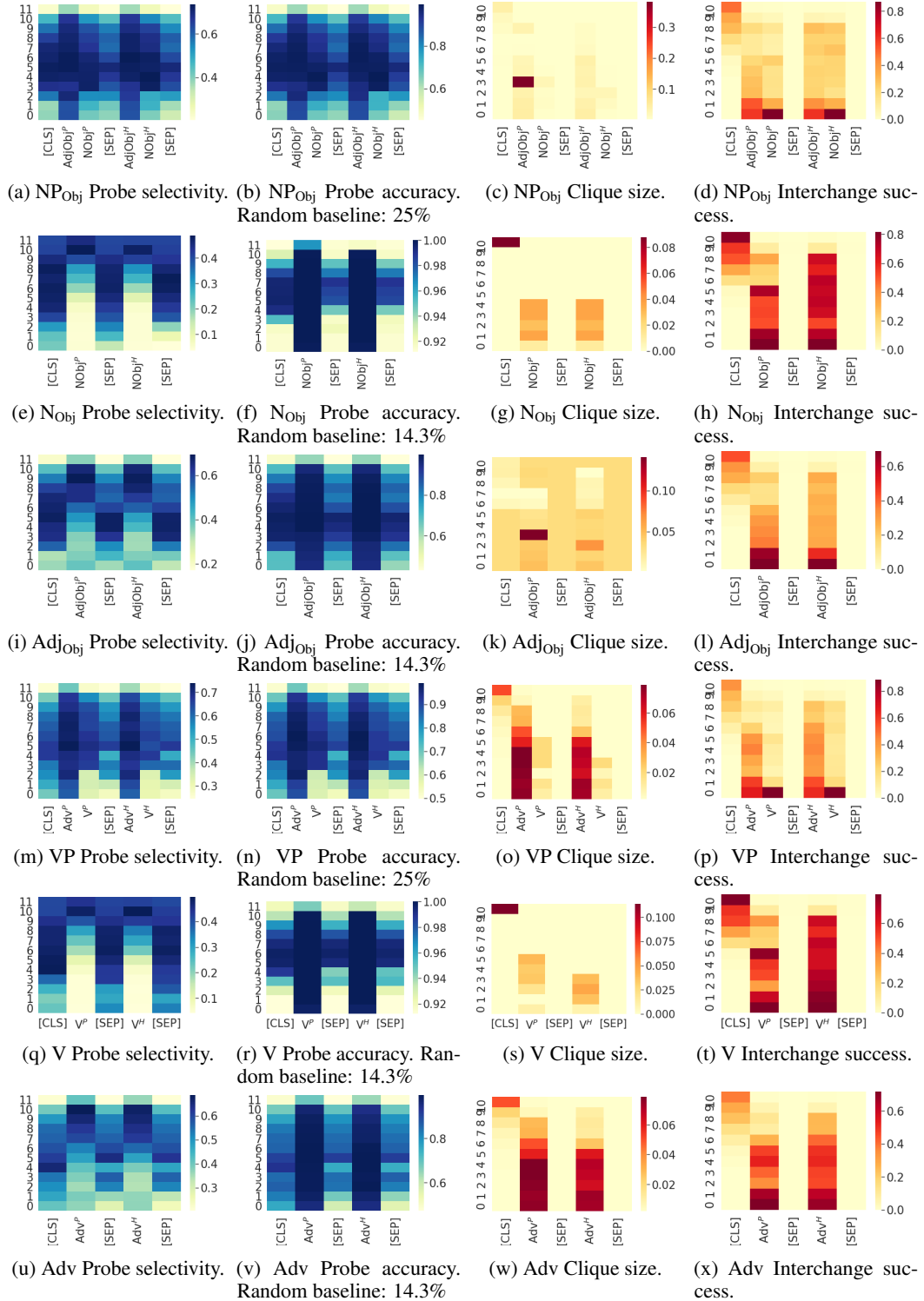


Figure 5: Full probing and interchange intervention results. Vertical axes denote layers of BERT and horizontal axes denote the token position of hidden representations. The intervention success rates reported here are calculated based on intervention experiments with a change in the output label. Clique sizes are reported as % of all examples.

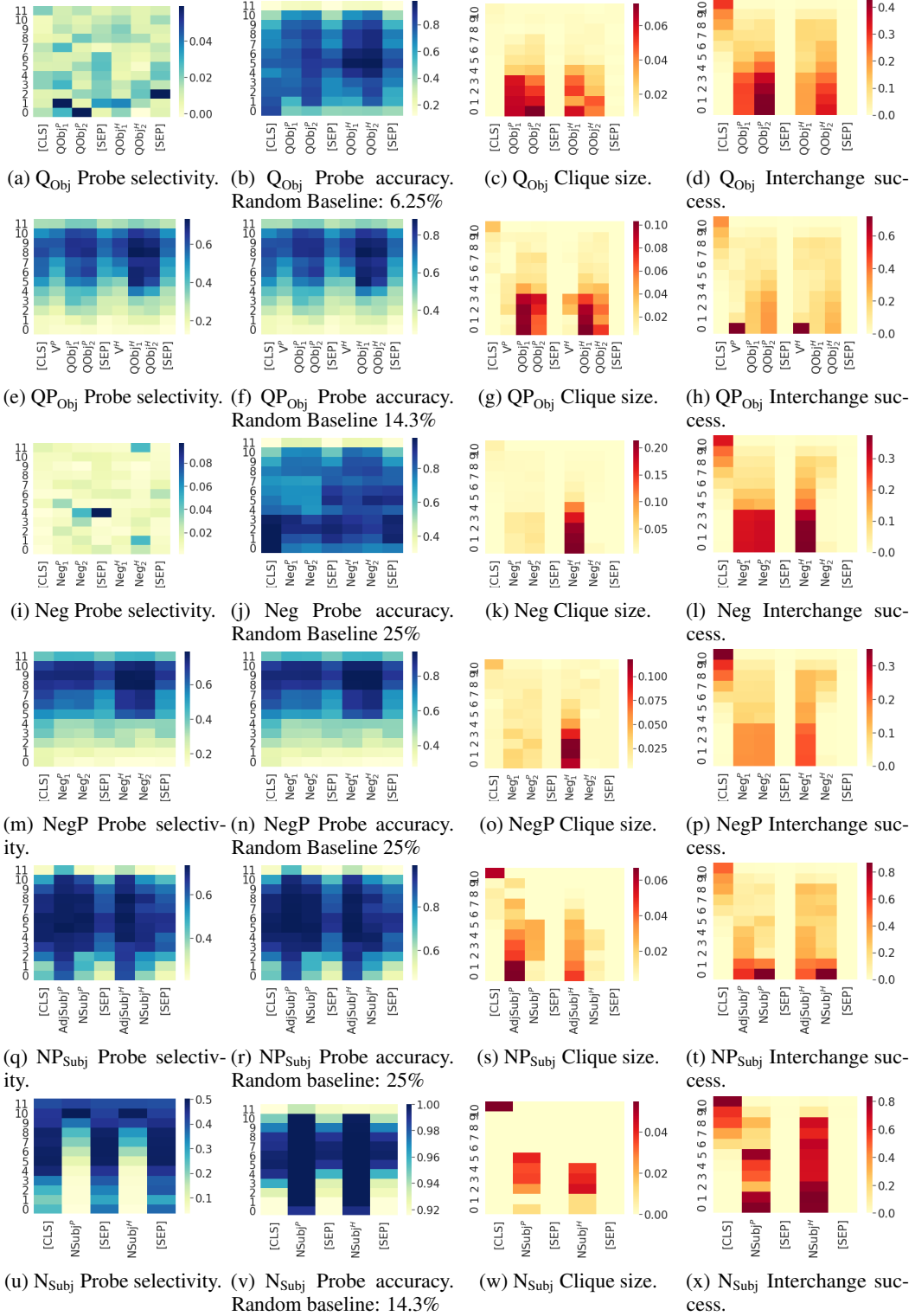


Figure 6: Full probing and interchange intervention results. Vertical axes denote layers of BERT and horizontal axes denote the token position of hidden representations. The intervention success rates reported here are calculated based on intervention experiments with a change in the output label. Clique sizes are reported as % of all examples.

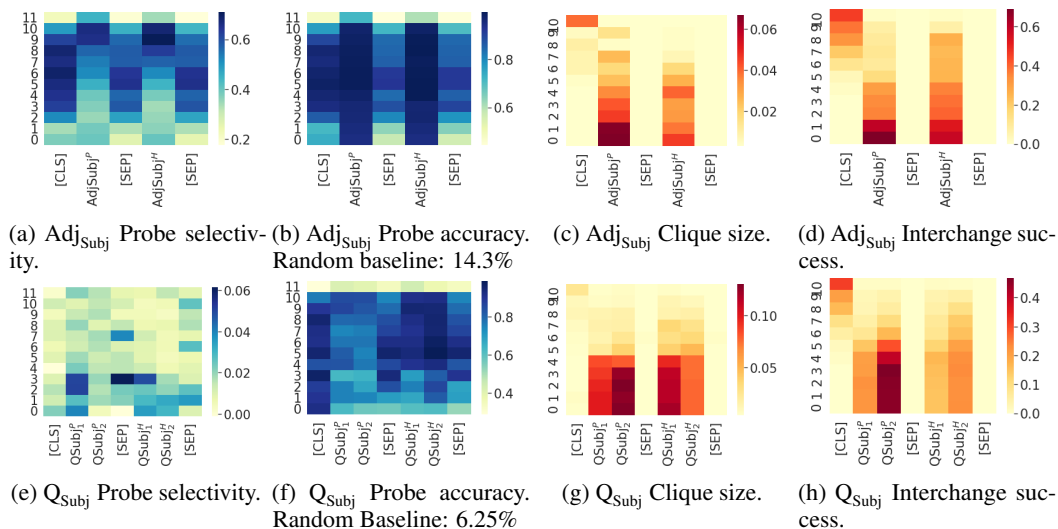


Figure 7: Full probing and interchange intervention results. Vertical axes denote layers of BERT and horizontal axes denote the token position of hidden representations. The intervention success rates reported here are calculated based on intervention experiments with a change in the output label. Clique sizes are reported as % of all examples.

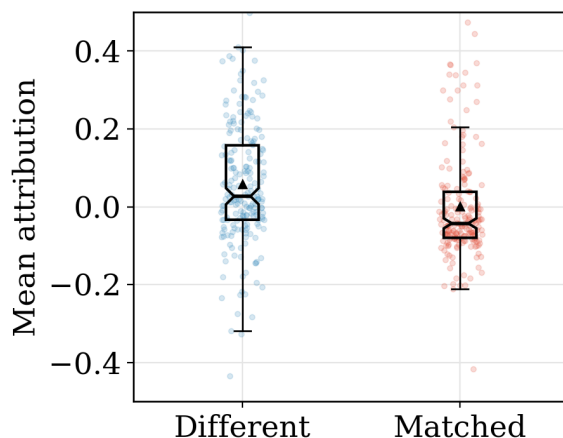


Figure 8: Integrated Gradients values for examples in which the premise and hypothesis differ by in exactly one aligned position. ‘Different’ refers to the IG value for this position, and ‘Matched’ is a randomly selected different position from each example. The two populations are different according to a Wilcoxon signed-rank test ($p < 0.00001$). The ‘Different’ positions positive on average, aligning with our expectation that they tend to be decisive for the output prediction.

E Integrated Gradients

We report attributions for the first BERT layer; later layers tend to concentrate importance onto the [CLS] token, since it is the direct basis for the classifier head in our model. To simplify the analysis, we restrict attention to examples in which exactly one position is different across the premise and hypothesis, and ‘Matched’ is a randomly selected position from elsewhere in the example. We see that the ‘Matched’ are positive in general, which aligns with our expectation that they are the most important positions in these examples.

F Probing Details

F.1 Probe Models

Our probe models are single-layer softmax classifiers: $y_i \propto \text{softmax}(Ah_i + b)$ where h_i is a hidden representation and $y_i \in \mathcal{R}$. To control the dimensionality of A , we factorize it in the form $A = LR$ where $L \in \mathbb{R}^{|\mathcal{R}| \times \ell}$ and $R \in \mathbb{R}^{\ell \times d}$ where d is the dimensionality of h_i .

We train the probes on hidden representations of a set of 12,800 examples that are randomly selected from the model’s original training set. We additionally take 2,000 examples to form a development set for early stopping. We filter out examples if the model’s final prediction is incorrect.

For training, we perform a grid search, maximizing for selectivity. We set a dropout of 0.1, and apply early stopping when the development set loss does not increase for 4 epochs. We train for a maximum of 40 epochs. We also anneal the learning rate by a factor of 0.5 if the dev set loss did not increase in the last epoch. We use a batch size of 512, learning rates in $\{0.001, 0.01\}$, weight decay regularization constants in $\{0.01, 0.1\}$. We set $\ell \in \{8, 32\}$ for restricting the maximum rank of the linear matrix A .

Using the same computation resources described above, each grid search setting took approximately 5 hours to run. For each grid search setting we trained a separate probe for every possible (causal model node, BERT representation) combination, where for the latter we use the intervention locations outlined in the “Alignment Search” part of Section 5.1 on each BERT layer.

F.2 Control Task

For each high-level node N , we construct a random mapping $\text{Control}_N : \mathcal{S}_N \mapsto \mathcal{L}_N$ where \mathcal{S} is the set of all aligned subexpressions under the node N and \mathcal{L}_N is the output label space. For phrasal nodes (VP, NegP, etc.) and aligned verbs and nouns, \mathcal{L}_N is the set of 7 possible relations $\{\#, \equiv, \sqsubset, \sqsupset, |, \wedge, \smile\}$ from MacCartney and Manning [2007]. For aligned quantifiers, the label space is the set of all projectivity signatures that can be produced by their composition.

Similar to Hewitt and Liang [2019], $\text{Control}_N(\cdot)$ will assign the same control label regardless of the context as long as its input consists of the same tokens. Consequently, the possible input space \mathcal{S}_N grows exponentially larger if N corresponds to longer subphrases (such as NegP and QP_{Obj}), and the control task becomes much more difficult to solve, resulting in accuracies around random selection.

F.3 Extended Probe Analysis

In Figure 7 we report some more representative selectivity and accuracy results for our probing experiments on BERT trained on the hard variant, juxtaposed against intervention experiments on the same model. For open-class words and full phrases, probing and intervention show similar trends. For aligned closed-class words, we find near-zero selectivity because the domain of the control function is so small. Figure 7 provides examples.

In general, probing and intervention experiments for relations between aligned single open-class words (i.e., N_{Subj} , Adj_{Subj} , N_{Obj} , Adj_{Obj} , Adv, V) show similar trends, which can be seen back in figures 6u to 6x. Every location except those above the [CLS] and [SEP] tokens has a near-100% accuracy, while selectivity is only high in the last few layers. Lower layers of BERT contains more information about word identity and hence may allow the probe to memorize each input pair, resulting in higher control task accuracy and lower selectivity for lower layers.

Probing experiments for relations between aligned multi-word subphrases (i.e., NP_{Subj} , VP, NP_{Obj} , QP_{Obj} and NegP) show similar trends as shown in the row of figures 6m to 6h. As described in Section F.2, all control probes for these achieve near-random performance so selectivity and accuracy differ by the random baseline accuracy, which is evident by comparing figures 6m and 6n.

On the other hand, probing experiments for aligned closed-class words (quantifiers and negation) have near-zero selectivity, as shown in Figure 6a. This is because the domain of the control function is the small set of closed-class word pairs, so memorizing the identity of these words becomes trivial for the probe.

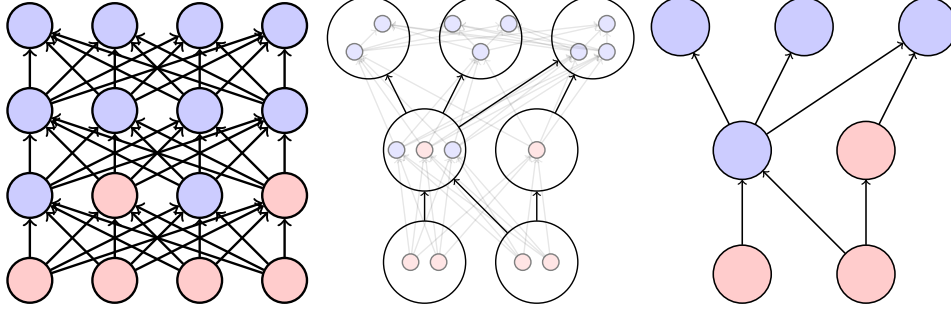


Figure 9: Schematic depicting constructive abstraction [Beckers and Halpern, 2019]. The variables of the low-level model (left) are divided into partitions (center) such that each low-level partition corresponds to a high level variable from the high-level model (right). The circles represent variables and the arrows represent causal dependencies. Blue circles are variables that are not being intervened on and red circles are variables that are being intervened on. Observe that a low-level causal dependence between partitions does not necessarily result in a high-level causal dependence between variables and that not every low-level intervention results in a high level intervention.

G Background on Causal Models and Causal Abstraction

In this appendix we provide relevant background on causal models and causal abstraction, sufficient to define the notion of *constructive abstraction*.

G.1 Causal Models

Definition G.1. (Signatures) A signature S is a pair $(\mathcal{V}, \mathcal{R})$, \mathcal{V} is a set of variables and \mathcal{R} is a function that associates with every variable $X \in \mathcal{V}$ a nonempty set $\mathcal{R}(X)$ of possible If $\mathbf{X} = (X_1, \dots, X_n)$, $\mathcal{R}(\mathbf{X})$ denotes the cross product $\mathcal{R}(X_1) \times \dots \times \mathcal{R}(X_n)$.

Definition G.2. (Causal models) A causal model M is a pair (S, \mathcal{F}) , where S is a signature and \mathcal{F} defines a function that associates with each variable X a structural equation \mathcal{F}^X giving the value of X in terms of the values of other variables. Formally, the equation \mathcal{F}^X maps $\mathcal{R}(\mathcal{V} - \{X\})$ to $\mathcal{R}(X)$, so \mathcal{F}^X determines the value of X , given the values of all the other variables in \mathcal{V} .

Definition G.3. (Dependence) X causes Y according to M , denoted $X \rightsquigarrow Y$, if there is some setting of the variables other than X and Y such that varying the value of X results in a variation in the value of Y ; that is, there is a setting \mathbf{z} of the variables $\mathbf{Z} = \mathcal{V} - \{X, Y\}$ and values x and x' of X $\mathcal{F}^Y(x, \mathbf{z}) \neq \mathcal{F}^Y(x', \mathbf{z})$.

Definition G.4. (Intervention) An intervention i has the form $\mathbf{X} \leftarrow \mathbf{x}$, where \mathbf{X} is a vector of variables. Intuitively, this means that the values of the variables in \mathbf{X} are set to \mathbf{x} . Setting the value of some variables $\mathbf{X} \leftarrow \mathbf{x}$ in a causal model $M = (S, \mathcal{F})$ results in a new causal model, denoted $i(M)$, which is identical to M , except that \mathcal{F} is replaced by $i(\mathcal{F})$: for each variable $Y \notin \mathbf{X}$, $i(\mathcal{F}^Y) = \mathcal{F}^Y$ (i.e., the equation for Y is unchanged), while for each $X' \in \mathbf{X}$, $i(\mathcal{F}^{X'}) = x'$ (where x' is the value in \mathbf{x} corresponding to x).

When we write out the structured equations for a variable X , for simplicity's sake, we treat \mathcal{F}^X as a map from $\mathcal{R}(\{Y \in \mathcal{V} : Y \rightsquigarrow X\})$ to $\mathcal{R}(X)$.

Note that interventions $\mathbf{X} \leftarrow \mathbf{x}$ corresponding 1-1 with variable settings \mathbf{x} . We make use of this in what follows.

G.2 Constructive Abstraction

The following definitions are in agreement with the definitions from Beckers and Halpern [2019], but differ somewhat in presentation. We additionally omit exogenous variables, as they play no role in our deterministic setting. In this section we take causal models to be pairs (M, \mathcal{I}) , with a set \mathcal{I} of *admissible interventions* made explicit.

Definition G.5. (Projection and Inverse Projection) Given some $\mathbf{v} \in \mathcal{R}(\mathcal{V})$ and $\mathbf{X} \subseteq \mathcal{V}$, define $Proj(\mathbf{v}, \mathbf{X})$ to be the restriction of \mathbf{v} to the variables in \mathbf{X} . Given some $\mathbf{x} \subseteq \mathcal{V}(\mathbf{X})$, the inverse

$Proj^{-1}(\mathbf{x})$ is defined as usual:

$$\{\mathbf{v} \in \mathcal{R}(\mathcal{V}) : \mathbf{x} \text{ is the restriction of } \mathbf{v} \text{ to } \mathbf{X}\}.$$

We are interested in (possibly partial) functions $\tau : \mathcal{R}_L(\mathcal{V}_L) \rightarrow \mathcal{R}_H(\mathcal{V}_H)$ mapping settings of low-level variables to settings of high-level variables. Such a function naturally induces a function between sets of interventions.

We are now in a position to define τ -abstraction:

Definition G.6. (τ -abstraction) Fix a function $\tau : \mathcal{R}_L(\mathcal{V}_L) \rightarrow \mathcal{R}_H(\mathcal{V}_H)$, which in turn fixes $\omega_\tau : \mathcal{I}_L \rightarrow \mathcal{I}_H$. We say (M_H, \mathcal{I}_H) is a τ -abstraction of (M_L, \mathcal{I}_L) if the following hold:

1. τ is surjective.
2. ω_τ is surjective.
3. for all $i_L \in \mathcal{I}_L$ we have $\tau(i_L(M_L)) = \omega_\tau(i_L)(M_H)$.

One way to think of this: τ is a map from $\mathcal{R}(\mathcal{V}_L)$ to $\mathcal{R}(\mathcal{V}_H)$, which in turn induces a map ω_τ from the space of *projections* on $\mathcal{R}(\mathcal{V}_L)$ to *projections* on $\mathcal{R}(\mathcal{V}_H)$. The conditions on τ -abstraction below then simply become that τ and ω_τ are both total and surjective on their respective (co)domains, and a second condition that can be easily encoded in terms of potential outcomes. For any setting/projection \mathbf{x} at the low-level, we require that $M_L \models \mathbf{v}_\mathbf{x}$ iff $M_H \models \tau(\mathbf{v})_{\omega_\tau(\mathbf{x})}$. Finally, to be a constructive τ -abstraction we simply require that τ decompose into a family of functions, as below.

Definition G.7. (Strong τ -abstraction) If M_H and M_L are basic causal models, then M_H is a strong τ -abstraction of M_L if \mathcal{I}_H^τ is the set of *all* high-level interventions, and $(M_H, \mathcal{I}_H^\tau)$ is a τ -abstraction of $(M_L, \mathcal{I}_L^\tau)$.

Definition G.8. (Constructive τ -abstraction) M_H is a constructive τ -abstraction of M_L if M_H is a strong τ -abstraction of M_L and there exists a partition $P = \{\bar{P}_{X_H} \text{ for } X_H \in \mathcal{V}_H \cup \{\emptyset\}\}$ of \mathcal{V}_L , where \bar{P}_{X_H} for $X_H \in \mathcal{V}_H$ are nonempty, and mappings $\tau_{X_H} : \mathcal{R}_L(\bar{P}_{X_H}) \rightarrow \mathcal{R}_H(X_H)$ for $X_H \in \mathcal{V}_H$ such that $\tau(\vec{v}_L) = \times_{X_H \in \mathcal{V}_H} \tau_{X_H}(\vec{p}_{X_H})$, where $\vec{p}_{X_H} = Proj(\vec{v}_L, \bar{P}_{X_H})$, and \times is the concatenation operator on sequences. M_H is a constructive abstraction of M_L if it is a constructive τ -abstraction of M_L for some τ . For any $X_H \in \mathcal{V}_H$ and $X_L \in \bar{P}_{X_H}$, there must exist distinct $x_H, x'_H \in \mathcal{R}_H(X_H)$ and distinct $x_L, x'_L \in \mathcal{R}_L(X_L)$ such that $\tau_{X_H}(\vec{p}_{X_H}) = x_H$ and $\tau_{X_H}(\vec{p}'_{X_H}) = x'_H$ for some \vec{p}_{X_H} and \vec{p}'_{X_H} consistent with x_L and x'_L , respectively.

An alternative, but equivalent definition would be:

Definition G.9 (Constructive τ -abstraction, second definition). (M_H, \mathcal{I}_H) is a constructive τ -abstraction of (M_L, \mathcal{I}_L) if, in addition to being a τ -abstraction, we can associate with each X_H a subset P_{X_H} of \mathcal{V}_L , such that the mapping $\tau : \mathcal{R}(\mathcal{V}_L) \rightarrow \mathcal{R}(\mathcal{V}_H)$ decomposes into a family of functions $\tau_{X_H} : \mathcal{R}(P_{X_H}) \rightarrow \mathcal{R}(X_H)$. We say M_H is a constructive abstraction of M_L if it is a constructive τ -abstraction for some τ .

In other words, for a constructive abstraction it suffices to define the component functions τ_{X_H} , as these completely determine τ . In fact, the maps τ_{X_H} more generally induce a (partial) function from projections of $\mathcal{R}(\mathcal{V}_L)$ to (in fact, onto) projections of $\mathcal{R}(\mathcal{V}_H)$ in the following sense. For any setting $\mathbf{h} = [h_1 \dots h_k]$ of high-level variables H_1, \dots, H_k we can find low-level setting \mathbf{y} such that projections of \mathbf{y} map via τ_{H_i} to h_i . Slightly abusing notation denote this (partial) low-level setting \mathbf{y} as $\tau^{-1}(\mathbf{h})$. So, in particular when \mathbf{h} corresponds to an intervention in \mathcal{I}_H , the setting $\tau^{-1}(\mathbf{h})$ should specify a corresponding intervention in \mathcal{I}_L . Indeed, point (2) of Def. G.6 tells us that (the intervention corresponding to) $\tau^{-1}(\mathbf{h})$ should be mapped via ω_τ to (the intervention corresponding to) \mathbf{h} .

H Causal Abstraction Analysis of C_+

H.1 Formal Definition of C_+

We define the causal model $C_+ = (\mathcal{V}_+, \mathcal{R}_+, \mathcal{F}_+)$ as follows (where $\mathbb{N}_k = \{0, \dots, k\}$):

$$\mathcal{V}_+ = \{D_1, D_2, D_3, D_4, S_1, S_2\}$$

$$\begin{aligned}\mathcal{R}_+(D_i) &= \mathbb{N}_9, \text{ for } i \in \{1, 2, 3, 4\} \\ \mathcal{R}_+(D_1) &= \mathcal{R}_+(D_2) = \mathcal{R}_+(D_3) = \mathcal{R}_+(D_4) = \mathbb{N}_9 \\ \mathcal{R}_+(S_1) &= \mathbb{N}_{18} \mathcal{R}_+(S_2) = \mathbb{N}_{27}\end{aligned}$$

$$\begin{aligned}\mathcal{F}_+^{D_1} &= \mathcal{F}_+^{D_2} = \mathcal{F}_+^{D_3} = 0 & \forall d \in \mathcal{R}(D_3) : \mathcal{F}_+^{D_4}(d) &= d \\ \forall (d, d') \in \mathcal{R}(D_1) \times \mathcal{R}(D_2) : \mathcal{F}_+^{S_1}(d, d') &= d + d' \\ \forall (s, d) \in \mathcal{R}(S_1) \times \mathcal{R}(D_4) : \mathcal{F}_+^{S_2}(s, d) &= s + d\end{aligned}$$

H.2 Formal Definition of N_+

In the main text, we did not provide a specific identity for N_+ . Here, we define N_+ to be a feed forward network, which we represent directly as a causal model $C_{N_+} = (\mathcal{V}_{N_+}, \mathcal{R}_{N_+}, \mathcal{F}_{N_+})$.

Let $W \in \mathbb{R}^{30 \times 3}$, for $k \in \{1, 3\}$ let $W_{jk} = j\%10$ if $0 \leq j \leq 20$, otherwise $W_{jk} = 0$, and let $W_{j2} = 0$ if $0 \leq j \leq 20$, otherwise $W_{j2} = j\%10$. Let $U \in \mathbb{R}^3$ and $U = [1, 1, 0]$.

$$\mathcal{V}_{N_+} = \{X_1, X_2, X_3, H_1, H_2, H_3, O\}$$

$$\begin{aligned}\mathcal{R}_{N_+}(X_1) &= \mathcal{R}_{N_+}(X_2) = \mathcal{R}_{N_+}(X_3) = \{0, 1\}^{10} \\ \mathcal{R}_{N_+}(O) &= \mathcal{R}_{N_+}(H_1) = \mathcal{R}_{N_+}(H_2) = \mathcal{R}_{N_+}(H_3) = \mathbb{R}\end{aligned}$$

$$\begin{aligned}\mathcal{F}_{N_+}^{X_1} &= \mathcal{F}_{N_+}^{X_2} = \mathcal{F}_{N_+}^{X_3} = 0 \\ \forall \mathbf{x} \in \mathcal{R}_{N_+}(X_1) \times \mathcal{R}_{N_+}(X_2) \times \mathcal{R}_{N_+}(X_3) : [\mathcal{F}_{N_+}^{H_1}(\mathbf{x}) \mathcal{F}_{N_+}^{H_2}(\mathbf{x}) \mathcal{F}_{N_+}^{H_3}(\mathbf{x})] &= \text{ReLU}(\mathbf{x}W) \\ \forall \mathbf{h} \in \mathcal{R}_{N_+}(H_1) \times \mathcal{R}_{N_+}(H_2) \times \mathcal{R}_{N_+}(H_3) : \mathcal{F}_{N_+}^O(\mathbf{h}) &= \text{ReLU}(\mathbf{h}U)\end{aligned}$$

This network uses one-hot representations $x_1, x_2, x_3 \in \{0, 1\}^{10}$ to represent inputs from \mathbb{N}_9 .

H.3 Proving C_+ is an abstraction of N_+

We now prove that C_+ is an abstraction C_{N_+}

We define the mapping $\tau : \mathcal{R}_{N_+}(\mathcal{V}_{N_+}) \rightarrow \mathcal{R}_+(\mathcal{V}_+)$ as follows. We first partition the variables of N_+ into cells: $P_{D_1} = \{X_1\}$, $P_{D_2} = \{X_2\}$, $P_{D_3} = \{X_3\}$, $P_{D_4} = \{H_2\}$, $P_{S_1} = \{H_1\}$, $P_{S_2} = \{H_3\}$, $P_\emptyset = \{H_3\}$. To define τ it suffices to define the component functions τ_V for $V \in \mathcal{V}_+$. Let $B : \{0, 1\}^{10} \rightarrow \mathbb{N}_9$ be the partial function s.t. $B([v_1, v_2, \dots, v_n]) = k$ if $v_k = 1$ and $v_j = 0$ for $j \neq k$. Set $\tau_{D_1}, \tau_{D_2}, \tau_{D_3}$ all equal to B , and let $\tau_{D_4}, \tau_{S_1}, \tau_{S_2}$ all be the identity function.

Let \mathcal{I}_+ be the set of all interventions on C_+ that determine values for (at least) D_1, D_2 , and D_3 . Let $\mathcal{I}_{N_+} = \text{dom}(\omega_\tau)$. I.e., \mathcal{I}_{N_+} includes exactly the (interventions corresponding to) projections of $\mathcal{R}_{N_+}(\mathcal{V}_{N_+})$ that map via ω_τ to some admissible intervention on C_+ . Because elements of \mathcal{I}_+ always determine values for D_1, D_2, D_3 , every intervention in \mathcal{I}_{N_+} determines a value for each of X_1, X_2, X_3 . In fact, these values are guaranteed to be in the domains of $\tau_{D_1}, \tau_{D_2}, \tau_{D_3}$, respectively.

We now prove the three conditions guaranteeing (C_+, \mathcal{I}_+) is a τ -abstraction of $(C_{N_+}, \mathcal{I}_{N_+})$.

(1) The first point is that the map τ is surjective. Take an arbitrary $(d_1, d_2, d_3, d_4, s_1, s_2) \in \mathcal{R}_+(\mathcal{V}_+)$. We determine an element of $\mathcal{R}_{N_+}(\mathcal{V}_{N_+})$ as follows: $x_k = B^{-1}(d_k)$ for $k \in \{1, 2, 3\}$, $[h_1 h_2 h_3] =$

$[s_1 d_2 s_1]$, and $o = s_2$. It's then clear that $\tau(x_1, x_2, x_3, h_1, h_2, h_3, o) = (d_1, d_2, d_3, d_4, s_1, s_2)$. As $(d_1, d_2, d_3, d_4, s_1, s_2)$ was chosen arbitrarily, τ is surjective.

(2) The second point is that ω_τ must also be surjective onto the set \mathcal{I}_+ of all interventions on C_+ . Any intervention $i_+ \in \mathcal{I}_+$ can be identified with a vector \mathbf{i}^+ of values of variables in \mathcal{V}_+ . By definition of \mathcal{I}_+ , i_+ fixes at least the values of D_1, D_2, D_3 . Consider the intervention i_{N_+} corresponding to $\mathbf{i}^{N_+} = \tau^{-1}(\mathbf{i}^+)$. It suffices to show that $\omega_\tau(i_{N_+}) = i_+$. In other words, we need to show that $Proj^{-1}(\mathbf{i}^{N_+}) = Proj^{-1}(\mathbf{i}^+)$.

First, we show for all $\mathbf{v}_L \in Proj^{-1}(\mathbf{i}^{N_+})$ that $\tau(\mathbf{v}_L) \in Proj^{-1}(\mathbf{i}^+)$. By construction of i_+ , any variables fixed by i_{N_+} will correspond (via τ component functions) to values of variables fixed by i_+ , except for the variable H_3 , which has no corresponding high level variable. We merely need to observe that for any values of variables *not* set by i_{N_+} , there exist corresponding values for the variables that are *not* set by i_+ , such that the appropriate τ component functions map the former to the latter (with the exception of H_3 , which has no corresponding high level variable). This is obvious from the definition of the components of τ .

Second, we show for all $\mathbf{v}_H \in Proj^{-1}(\mathbf{i}^+)$ there is $\mathbf{v}_L \in Proj^{-1}(\mathbf{i}^{N_+})$ such that $\tau(\mathbf{v}_L) = \mathbf{v}_H$. Again, by construction of i_+ , any variables fixed by i_+ will correspond (via τ component functions) to values of variables fixed by i_{N_+} . We merely need to observe that for any values of variables *not* set by i_+ , there exist corresponding values for the variables *not* set by i_{N_+} , such that the appropriate τ component functions map the former to the latter, with H_3 taking on any value. This is obvious from the definition of the components of τ . This concludes the argument that $\omega_\tau(i_{N_+}) = i_+$.

(3) Finally, we need to show for each $i_{N_+} \in dom(\omega_\tau)$ that $\tau(i_{N_+}(C_{N_+})) = \omega_\tau(i_{N_+})(C_+)$. The point here is that the two causal processes unfold in the same way, under any intervention.

Indeed, pick any i_{N_+} and suppose that $i_+ = \omega_\tau(i_{N_+})$. We know that i_+ fixes values d_1, d_2, d_3 of D_1, D_2, D_3 , and likewise that i_{N_+} fixes values x_1, x_2, x_3 of X_1, X_2, X_3 such that $\tau_{D_i}(x_i) = d_i$ for $i \in \{1, 2, 3\}$. Any other variables fixed by i_+ from among D_4, S_1, S_2 will likewise correspond (via $\tau_{D_4}, \tau_{S_1}, \tau_{S_2}$) to values of H_2, H_1, O fixed by i_{N_+} . We merely need to observe that any variables that are *not* set by i_+ and i_{N_+} will still correspond via the appropriate τ -component, given their settings in $i_+(C_+)$ and $i_{N_+}(C_{N_+})$. The mechanisms in C_{N_+} were devised precisely to guarantee this.

Thus we have fulfilled the three requirements and we have shown that C_+ is an abstraction C_{N_+} .

The proof that C_{NatLog} is a constructive abstraction of N_{NLI} follows this same pattern.

I Causal Abstraction Analysis of C_{NatLog}

I.1 Formal Definition of C_{NatLog}

We formally define the model $C_{NatLog} = (\mathcal{V}_{NatLog}, \mathcal{R}_{NatLog}, \mathcal{F}_{NatLog})$ as follows.

$$\mathcal{V}_{NatLog} = \{Q_{Subj}^P, Q_{Subj}^H, Adj_{Subj}^P, Adj_{Subj}^H, N_{Subj}^P, N_{Subj}^H, Neg^P, Neg^H, Adv^P, Adv^H,$$

$$V^P, V^H, Q_{Obj}^P, Q_{Obj}^H, Adj_{Obj}^P, Adj_{Obj}^H, N_{Obj}^P, N_{Obj}^H, Q_{Subj}, Adj_{Subj}, N_{Subj}, Neg, Adv, V,$$

$$Q_{Obj}, Adj_{Obj}, N_{Obj}, NP_{Subj}, VP, NP_{Obj}, QP_{Obj}, NegP, QP_{Subj}\}$$

$$\begin{aligned}
\mathcal{R}_{NatLog}(Q_{Subj}^P) &= \mathcal{R}_{NatLog}(Q_{Subj}^H) = \mathcal{R}_{NatLog}(Q_{Subj}^H) = \mathcal{R}_{NatLog}(Q_{Subj}^H) \\
&= \{no, some, every, notevery\} \\
\mathcal{R}_{NatLog}(Neg^P) &= \mathcal{R}_{NatLog}(Neg^H) = \{not, \epsilon\} \\
\mathcal{R}_{NatLog}(Adj_{Subj}^P) &= \mathcal{R}_{NatLog}(Adj_{Subj}^H) = \mathbf{Adj}_{Subj} \\
\mathcal{R}_{NatLog}(N_{Subj}^P) &= \mathcal{R}_{NatLog}(N_{Subj}^H) = \mathbf{N}_{Subj} \\
\mathcal{R}_{NatLog}(Adv^P) &= \mathcal{R}_{NatLog}(Adv^H) = \mathbf{Adv}_{Subj} \\
\mathcal{R}_{NatLog}(V^P) &= \mathcal{R}_{NatLog}(V^H) = \mathbf{V}_{Subj} \\
\mathcal{R}_{NatLog}(Adj_{Obj}^P) &= \mathcal{R}_{NatLog}(Adj_{Obj}^H) = \mathbf{Adj}_{Obj} \\
\mathcal{R}_{NatLog}(N_{Obj}^P) &= \mathcal{R}_{NatLog}(N_{Obj}^H) = \mathbf{N}_{Obj} \\
\mathcal{R}_{NatLog}(Q_{Obj}) &= \mathcal{R}_{NatLog}(Q_{Subj}) = \mathcal{Q} \\
\mathcal{R}_{NatLog}(Neg) &= \mathcal{N} \\
\mathcal{R}_{NatLog}(Adj_{Obj}) &= \mathcal{R}_{NatLog}(Adj_{Subj}) = \mathcal{R}_{NatLog}(Adv) = \mathcal{A} \\
\mathcal{R}_{NatLog}(N_{Obj}) &= \mathcal{R}_{NatLog}(N_{Subj}) = \mathcal{R}_{NatLog}(V) = \{\#, \equiv\} \\
\mathcal{R}_{NatLog}(NP_{Subj}) &= \mathcal{R}_{NatLog}(NP_{Obj}) = \mathcal{R}_{NatLog}(VP) = \{\#, \equiv, \sqsubset, \sqsupset\} \\
\mathcal{R}_{NatLog}(QP_{Obj}) &= \mathcal{R}_{NatLog}(Neg^P) = \mathcal{R}_{NatLog}(QP_{Subj}) = \{\#, \equiv, \sqsubset, \sqsupset, |, \wedge, \smile\} \\
\mathcal{F}_N &= \mathbf{COMP} \text{ for } N \in \{VP, NP_{Subj}, NP_{Obj}, Neg^P, QP_{Obj}, QP_{Subj}\} \\
\mathcal{F}_N &= \mathbf{REL} \text{ for } N \in \{V, N_{Subj}, N_{Obj}\} \\
\mathcal{F}_N &= \mathbf{PROJ} \text{ for } N \in \{Q_{Obj}, Q_{Subj}, Adv, Adj_{Subj}, Adj_{Obj}, Neg\}
\end{aligned}$$

The set $\{\#, \equiv, \sqsubset, \sqsupset, |, \wedge, \smile\}$ contains the seven relations used in the natural logic of MacCartney and Manning [2007]. The set \mathbf{N}_{Subj} contains the subject nouns used to create MQNLI, \mathbf{N}_{Obj} the set of object nouns, \mathbf{Adj}_{Subj} the subject adjectives, \mathbf{Adj}_{Obj} the object adjectives, \mathbf{V} the verbs, and \mathbf{Adv} the adverbs. Additionally, \mathcal{Q} is the set of joint projectivity signatures between *every*, *some*, *not every*, and *no*, \mathcal{N} is the set of joint projectivity signatures between *not* and ϵ , \mathcal{A} is the set of joint projectivity signatures between intersective adjectives and adverbs and ϵ . $\mathbf{REL}(x, y)$ outputs the lexical relation between x and y . Finally, $\mathbf{COMP}(f, x_1, x_2, \dots, x_n) = f(x_1, x_2, \dots, x_n)$ and $\mathbf{PROJ}(f, g) = P_{f/g}$ where $P_{f/g}$ is the joint projectivity signature between f and g . See Geiger et al. [2019] for details about these sets and functions.

I.2 Formal Definition of C_{NatLog}^N

For some non-leaf node N of the tree in Figure 2, we define C_{NatLog}^N to be the marginalization of C_{NatLog} where all variables are removed other than the input variables

$$\mathcal{V}_{NatLog}^{Input} = Q_{Subj}^P, Q_{Subj}^H, Adj_{Subj}^P, Adj_{Subj}^H, N_{Subj}^P, N_{Subj}^H, Neg^P, Neg^H, Adv^P, Adv^H, V^P, V^H, \\
Q_{Obj}^P, Q_{Obj}^H, Adj_{Obj}^P, Adj_{Obj}^H, N_{Obj}^P, N_{Obj}^H$$

, the output variable QP_{Subj} and the intermediate variable N . For a definition of marginalization, see Bongers et al. [2020].

I.3 Formal definition of N_{NLI}

In the main text, N_{NLI} could represent either our BERT model or our LSTM model. We will maintain this ambiguity, because while these two models are drastically different at the highest level of detail, for the sake of our analysis we can view them both as creating a grid of neural representations where each representation in the grid is caused by all representations in the previous row and causes all representations in the following row. We will now formally define the causal model C_{NLI} .

$$\mathcal{V}_{N_{NLI}} = \{R_{11}, R_{12}, \dots, R_{1m}, \dots, R_{nm}, O\}$$

For the LSTM model $n = 2$ and for the BERT model $n = 12$. m is the number of tokens in a tokenized version of an MQNLI example.

$$\mathcal{R}_{N_{NLI}}(R_{jk}) = \mathbb{R}^d \quad \mathcal{R}_{N_{NLI}}(O) = \{\text{entailment, contradiction, neutral}\}$$

For all j and k and where d is the dimension of the vector representations.

$$\begin{aligned} \forall (r_{(j-1)1}, r_{(j-1)2}, \dots, r_{(j-1)m}) \in \mathcal{R}_{N_{NLI}}(R_{(j-1)1} \times R_{(j-1)2} \times \dots \times R_{(j-1)m}) \\ \mathcal{F}_{N_{NLI}}^{R_{jk}}(r_{(j-1)1}, r_{(j-1)2}, \dots, r_{(j-1)m}) = \mathbf{NN}_{jk}(r_{(j-1)1}, r_{(j-1)2}, \dots, r_{(j-1)m}) \end{aligned}$$

where \mathbf{NN}_{jk} is either the LSTM function or the BERT function that creates the neural representation at the j th row and k th column.

$$\forall r_{n1} \in \mathcal{R}_{N_{NLI}}(R_{n1}) \mathcal{F}_{N_{NLI}}^O(r_{n1}) = \mathbf{NN}_O(r_{n1})$$

where \mathbf{NN}_O is the neural network that makes a three class prediction using the final representation of the [CLS] token.

See Appendix C for details about these functions.

I.4 Proving C_{NatLog}^N is an abstraction of N_{NLI}

We will now formally prove that that C_{NatLog}^N is a constructive abstraction of N_{NLI} if the following holds for all $e, e' \in MQNLI$ where the representation location L is equivalent to the variable R_{jk} for some j and k . This would mean that every single one of our intervention experiments at this location are successful.

$$C_{NatLog}^{N \leftarrow e'}(e) = N_{NLI}^{L \leftarrow e'}(e) \quad (10)$$

We define the mapping $\tau : \mathcal{R}_{N_{NLI}}(\mathcal{V}_{N_{NLI}}) \rightarrow \mathcal{R}_{NatLog}^N(\mathcal{V}_{NatLog})$ as follows. We first partition the "low level" variables of N_{NLI} into partition cells.

$$\begin{aligned} P_N &= \{L\} & P_{QP_{Subj}} &= \{O\} \quad \forall X \in \mathcal{V}_{NatLog}^{Input} \\ P_X &= \{R_{1j}, R_{1(j+1)}, \dots, R_{1(j+k)}\} \end{aligned}$$

where $R_{1j}, R_{1(j+1)}, \dots, R_{1(j+k)}$ are the token vectors associated with the input variable X . Some of our causal model's input variables are tokenized into several tokens (See Appendix C for details).

To define τ , it then suffices to define the component functions τ_V for each $V \in \mathcal{V}_{NatLog}$. Let $T : (\mathbb{R}^d)^+ \rightarrow \mathcal{V}_{NatLog}^{Input}$ be the partial function mapping sequences of token vectors to the input variable they correspond to, where $+$ is the Kleene plus operator. Let $P : \mathcal{R}^3 \rightarrow \{\text{entailment, neutral, contradiction}\}$ be the partial function mapping a vector of logits to the output prediction they correspond to. Finally, let $Q_L : \mathbb{R}^d \rightarrow \mathcal{R}_{NatLog}(N)$ be the partial function such that for all $e \in MQNLI$, if \mathbf{v} is the vector created by N_{NLI} at location L when processing input e and x is the value realized by C_{NatLog} for the variable N when processing input e , then $Q_L(\mathbf{v}) = x$.

For all $\forall X \in \mathcal{V}_{NatLog}^{Input}$, we set τ_X to be T . We additionally set τ_N to be Q_L and $\tau_{QP_{Subj}}$ to be P .

Let \mathcal{I}_{NatLog} be the set of all interventions on C_{NatLog} that intervene on (i.e., determine the values for) at least the elements of $\mathcal{V}_{NatLog}^{Input}$. Let $\mathcal{I}_{N_{NLI}}$ be the set of interventions that is the domain of the partial function ω_τ . In other words, $\mathcal{I}_{N_{NLI}}$ includes exactly the projections of $\mathcal{R}_{N_{NLI}}(\mathcal{V}_{N_{NLI}})$ that map via ω_τ to some intervention on C_+ . The fact that P, Q_L, T are all proper partial functions prevent $\mathcal{I}_{N_{NLI}}$ from including all possible interventions on $C_{N_{NLI}}$.

We now prove the three conditions that must hold for $(C_{NatLog}, \mathcal{I}_{NatLog})$ to be a τ -abstraction of $(C_{N_{NLI}}, \mathcal{I}_{N_{NLI}})$.

(1) The first point is to show the map τ is surjective. So take an arbitrary element $(\vec{v}^{input}, n, q) \in \mathcal{R}_{NatLog}(\mathcal{V}_{NatLog})$. We specify an element of $\mathcal{R}_{N_{NLI}}(\mathcal{V}_{N_{NLI}})$ as follows:

$$\begin{aligned} l &= Q_L^{-1}(n) & o &= P^{-1}(q) \\ \forall v^{input} \in \vec{v}^{input} T^{-1}(v^{input}) &= (r_{1j}, r_{1(j+1)}, \dots, r_{1(j+k)}) \end{aligned}$$

where $r_{1j}, r_{1(j+1)}, \dots, r_{1(j+k)}$ are the token vectors corresponding to the input variable v^{input} .

It's then patent that $\tau(r_{11}, \dots, r_{n1}, r_{12}, \dots, r_{nm}, o) = (\vec{v}^{input}, n, q)$. As (\vec{v}^{input}, n, q) was chosen arbitrarily, we have shown τ is surjective.

(2) The second point is that ω_τ must also be surjective onto the set \mathcal{I}_{NatLog} of interventions on C_{NatLog} . Any intervention $i_{NatLog} \in \mathcal{I}_{NatLog}$ can be identified with a vector \mathbf{i}^{NatLog} of values of variables in \mathcal{V}_{NatLog} . By the definition of \mathcal{I}_{NatLog} , i_{NatLog} fixes the values of the variables in V^{input} and may also determine N and/or QP_{Subj} . Consider the intervention $i_{N_{NLI}}$ corresponding to $\mathbf{i}^{N_{NLI}} = \tau^{-1}(\mathbf{i}^{NatLog})$ as described in Section G.2. It suffices to show that $\omega_\tau(i_{N_{NLI}}) = i_{NatLog}$. In other words, we need to show parts 1, 2, and 3 from Def. ??.

Part 1 is clear, since by the definition of \mathcal{I}_{NatLog} we are guaranteed that \mathbf{i}^{NatLog} determines values for \mathbf{V}^{input} , and hence $\mathbf{i}^{N_{NLI}}$ fixes values for R_{11}, \dots, R_{1m} in the domains of $\tau_{V^{input}}$ for $V \in \mathbf{V}^{input}$. Then any intervention that intervenes only on the values of

Part 2 requires that for every $\mathbf{v}_{N_{NLI}} \in Proj^{-1}(\mathbf{i}^{N_{NLI}})$, we have $\tau(\mathbf{v}_{N_{NLI}}) \in Proj^{-1}(\mathbf{i}^{NatLog})$. Because of how we defined i_{NatLog} , any variables fixed by $i_{N_{NLI}}$ will correspond (via τ component functions) to values of variables fixed by i_{NatLog} , except for the variables $R_{jk} \notin \mathbf{V}^{input} \cup \{L\}$, which have no corresponding high level variables. We merely need to observe that, for any values for the variables that are *not* set by $i_{N_{NLI}}$, there exists corresponding values for the variables that are *not* set by i_{NatLog} such that the appropriate τ component functions map the former to the latter, except for the variables $R_{jk} \notin \mathbf{V}^{input} \cup \{L\}$, which, again, have no corresponding high level variables. This is plainly obvious from the definition of the components of τ .

Part 3 requires that for any $\mathbf{v}_{NatLog} \in Proj^{-1}(\mathbf{i}^{NatLog})$, there exists a $\mathbf{v}_{N_{NLI}} \in Proj^{-1}(\mathbf{i}^{N_{NLI}})$ such that $\tau(\mathbf{v}_{N_{NLI}}) = \mathbf{v}_{NatLog}$. Again, because of how we defined i_{NatLog} , any variables fixed by i_{NatLog} will correspond (via τ component functions) to values of variables fixed by $i_{N_{NLI}}$. We merely need to observe that for any values for the variables that are *not* set by i_{NatLog} , there exists corresponding values for the variables that are *not* set by $i_{N_{NLI}}$, such that the appropriate τ component functions map the former to the latter, with $R_{jk} \notin \mathbf{V}^{input} \cup \{L\}$ taking on any value. This is plainly obvious from the definition of the components of τ .

Thus, we have shown that $\omega_\tau(i_{N_{NLI}}) = i_{NatLog}$.

(3) Finally, we need to show for each $i_{N_{NLI}} \in dom(\omega_{tau})$ that $\tau(i_{N_{NLI}}(C_{N_{NLI}})) = \omega_\tau(i_{N_{NLI}})(C_{NatLog})$. The point here is that the two causal processes unfold in the same way, under any intervention. Indeed, pick any $i_{N_{NLI}}$ and suppose that $i_{NatLog} = \omega_\tau(i_{N_{NLI}})$. We know that i_{NatLog} fixes values for the variables in \mathbf{V}^{input} , and likewise that $i_{N_{NLI}}$ fixes values for the variables R_{11}, \dots, R_{1m} . Any other variables fixed by i_{NatLog} from among N, QP_{Subj} will likewise correspond (via the component functions of τ) to values of L and O . We merely need to observe that any variables that are *not* set by i_{NatLog} and $i_{N_{NLI}}$ will still correspond via the appropriate τ -component, given their settings in $i_{NatLog}(C_{NatLog})$ and $i_{N_{NLI}}(C_{N_{NLI}})$. The intervention experiments on N_{NLI} that we are assuming were successful were devised precisely to guarantee this.

We have thus fulfilled the three requirements and shown that C_{NatLog} is an abstraction of $C_{N_{NLI}}$.